UFL/COEL-92/009

Flow and Transport Characteristics at a Canal Network Burnt Store Isles, Punta Gorda, Florida

by

Hsiang Wang
Jung L. Lee
Lihwa Lin

June, 1992

Prepared for

City of Punta Gorda, Florida

REPORT DOCUMENTATION PAGE

1. Report No.	2.	3. Recipient's Accession No.

4. Title and Subtitle
FLOW and TRANSPORT CHARACTERISTICS at a CANAL NETWORK BURNT STORE ISLES, PUNTA GORDA, FLORIDA

5. Report Date
June 20, 1992

6.

7. Author(s)
Hsiang Wang, Jung L. Lee, Lihwa Lin

8. Performing Organization Report No.
UFL/COEL-92/009

9. Performing Organization Name and Address
Coastal and Oceanographic Engineering Department
University of Florida
336 Weil Hall
Gainesville, FL 32611

10. Project/Task/Work Unit No.

11. Contract or Grant No.

12. Sponsoring Organization Name and Address
Public Works Department, City of Punta Gorda
900 West Henry Street
Punta Gorda, FL 33950

13. Type of Report
Final

14.

15. Supplementary Notes

16. Abstract

A field measurement study augmented with numerical modeling was carried out for the determination of the flow and transport characteristics of a canal network in Section 15, Burnt Store Isles of Punta Gorda, Florida. The emphasis of the study is to assess the effects of a boat lock closure or opening to the Section 15 from the Alligator Creek. The amount of sediment and pollutant through the lock are also estimated.

The flow network in Section 15 is an integral part connecting with Alligator Creek to Charlotte Bay through several outlet openings. The network is mainly tidal dominated and only three outlets are important and responsible for flow and pollutant exchanges between the network and Alligator Creek. The three outlets are the boat lock in the middle of western boundary of the network, a mosquito ditch on the southside and a shallow opening north of the boat lock.

The boat lock is found to be responsible for water and pollutant exchanges for the central 5/8 portion of Section 15. In terms of time average flow rate, by closing the lock the contribution from Section 15 to the total discharge realizes a mere 3.5% reduction. Therefore, the boat lock is ineffective of trapping either sediment or pollutant with in the network. Closing the boat lock for an extended period will likely accelerate shoaling in the central portion of the network canal and to increase the average resident time of pollutant in the network, which could cause the pollutant to transport further upstream to the north portion of the network.

17. Originator's Key Words	18. Availability Statement
Boat lock Flow exchange Pollutant transport	

19. U. S. Security Classif. of the Report	20. U. S. Security Classif. of This Page	21. No. of Pages	22. Price
Unclassified	Unclassified	67	

PREFACE

This report presents results of field measurements and numerical modeling of the hydrodynamic and sedimentary behaviors at a boat lock located in Section 15, Burnt Store Isles of Punta Gorda, Florida. The purpose of the study is to establish the quantities of tidal flows through the lock in comparison with the flows bypassing the lock through other outlets between Section 15 and the Alligator Creek. The amount of sediment and pollutant transporting through the lock are also estimated in the study.

The research in this report is sponsored by the City of Punta Gorda. The study and the report were prepared by the Department of Coastal and Oceanographic Engineering, University of Florida.

Special appreciation is due to Mr. Thomas M. Wilcox, former deputy director of Public Works, and Mr. Mark Gronceski, former city environmental engineer, for their preparation and technical assistance of this research project in the initial stage. Other personnel at City Public Works Department including Mr. James Stillwell, Mr. Richard Bensen and Ms. Diana Lester also provided their support at various stages of the study. Appreciation is also due to Dr. G. Miao and Mr. T. Kim in the Coastal Engineering Department, University of Florida, for their participation in the field experiments.

Contents

List of Figures

List of Tables

Flow and Transport Characteristics at a Canal Network,
Burnt Store Isles, Punta Gorda, Florida

1 Introduction

The boat lock where the study was conducted is located in Section 15, Burnt Store Isles, Punta Gorda, Florida. This Section consists of residential subdivisions along a canal network and a golf course country club (Figure 1). Practically all the residential units are fronted with canals. As can be seen all the finger canals eventually enter a main trunk which forms a belt around the western boundary of the subdivision. This trunk canal has two main outlets and several small outlets. Of the two main outlets one is located on the south side and the other is on the north side. The south side outlet is a man-made mosquito ditch which connects to the Alligator Creek south of Section 15. The north side outlet, which connects to the north fork of the Alligator Creek (North Alligator Creek) is a maintained channel with a boat lock. This boat-lock channel provides the only navigable access for this subdivision to Charlotte Harbor via the north fork of the Alligator Creek. During the course of the study, a shallow ditch just north of the boat lock was also found to be an important outlet to the north branch of the creek.

For concerns about pollutants from the canal network being carried into the Alligator Creek through the lock, it is currently allowed to open only during the period of November 15 to May 15 when the discharge is thought to be small. During the remaining six months the lock is kept closed and boat transits have to go through the normal lock operation. This is not only inconvenient to the boaters but also adds financial burden to the City of Punta Gorda for lock maintenance.

Since the entire subdivision is bordered by marshes with a number of other openings to the Alligator Creek, it is not clear the role of the lock to the pollutant transport.

The main purpose of this study is to establish the quantity of flows through the lock in comparison with the amount by-passing the lock by flows through mosquito ditch and/or directly overland to and from the Alligator Creek. The rate of sediment and pollutant transports through the lock are also estimated in the study.

The study was accomplished through field measurements augmented with numerical models.

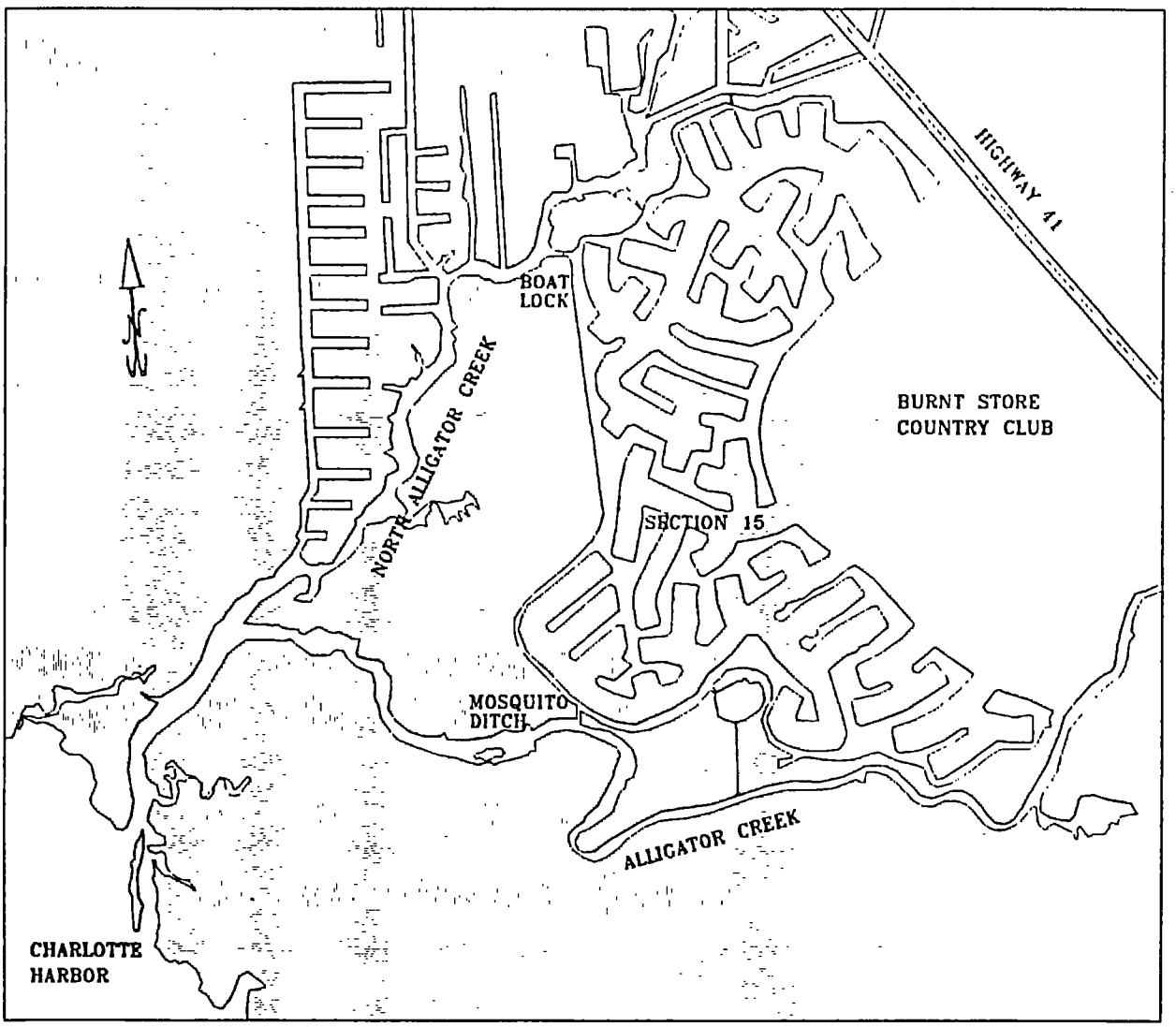

Figure 1: Alligator Creek and Section 15, Burnt Store Isles, Punta Gorda, Florida.

2 Field Study

Field measurements were conducted in the summer from July 24th to August 2nd, 1991, and again during the winter from January 15th to 24th, 1992. In May 1992, a brief drogue tracking study was conducted aimed at determining the flow patterns in the trunk canal in Section 15.

In the summer measurements, three tide gages were installed, one in Section 15, just directly across the boat lock, another at mosquito ditch connecting the canal system to the Alligator Creek and the third at Channel Marker 24 near junction of the Alligator Creek and its north fork branch. These locations are shown in Figure 2. Current measurements were carried out at seven cross-sections designated as Stations 1 to 7 shown in Figure 2. Here, Station 1 measures the flow in the north branch of the main canal trunk; Station 2 measures the flow in the south branch of the main canal trunk; Station 3 is at the throat of the boat lock; Stations 4, 5, and 6 are located in the north fork branch of Alligator Creek and Station 7 measures the combined flow from Alligator Creek and its north branch. Bottom sediment samples were also taken in the lock vicinity.

In the winter measurements, three tide gages were installed at the same locations as the summer experiment. In addition, two PUV gages were installed, one at the throat of the lock and the other at Station 6. The PUV gages measures the pressure (P) and current components in two perpendicular directions (U and V). The water surface fluctuations were also established from these pressure measurements. Current measurements were again carried out at the same seven cross-sections as the summer experiment, and sand samples were taken near the lock. Dispersion studies were also carried out at the lock. The experiment was performed by injecting Rhodamine dye at the lock in the beginning of the flood tidal cycle on January 21 and continuously monitoring its concentrations for a duration of two full days (four tidal cycles). The complete experimental deployment is also shown in Figure 2.

3 Results from Field Measurements

3.1 Summer Measurements

The water surface level fluctuation histories at the three tide gage locations from the summer measurements are plotted in Figure 3. The variations are mainly tidal induced as there was no major storm or runoff event occurred during the measurement period. The tidal action in the study area is a mixture of diurnal

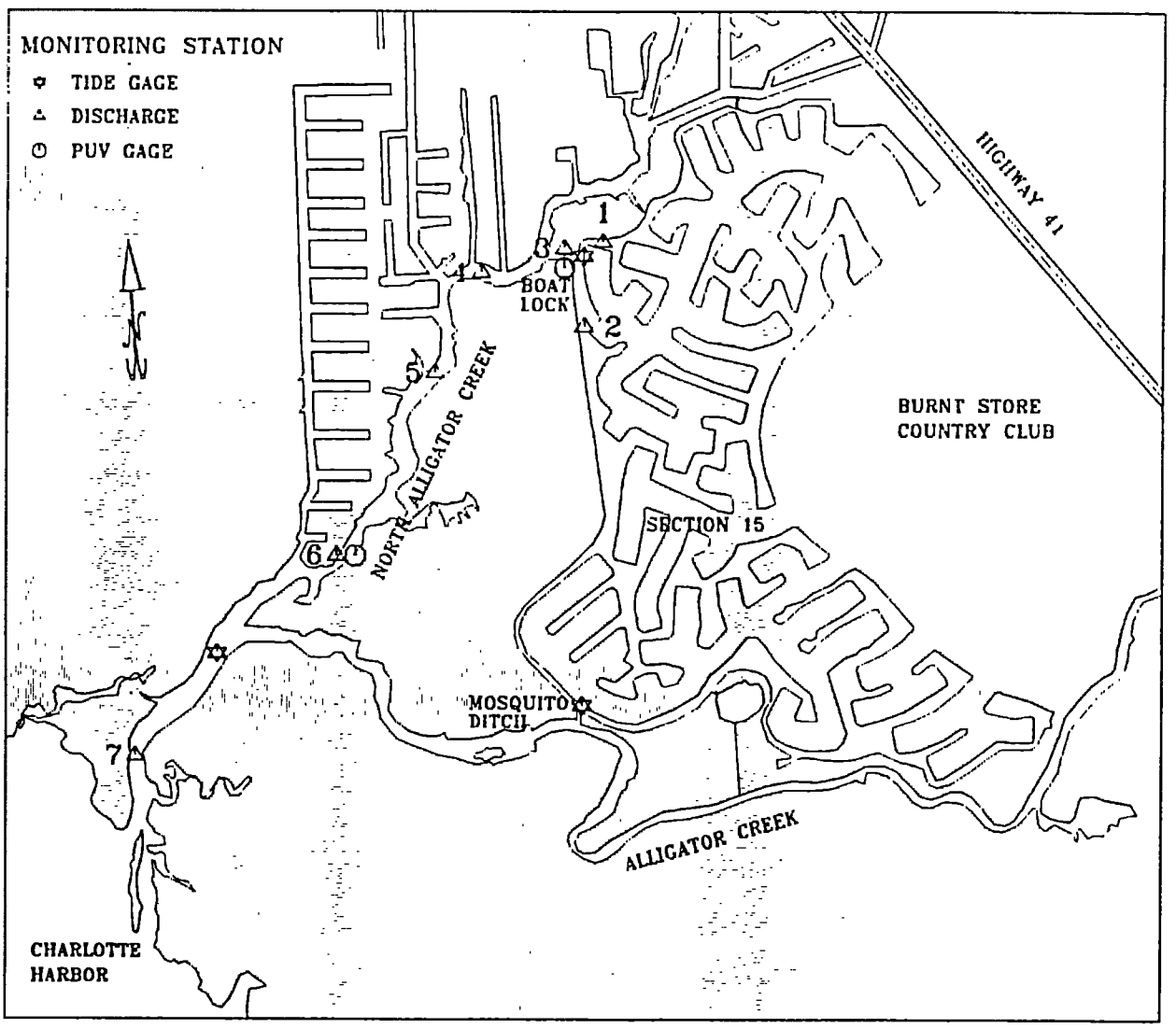

Figure 2: Instrument stations and experimental deployment locations.

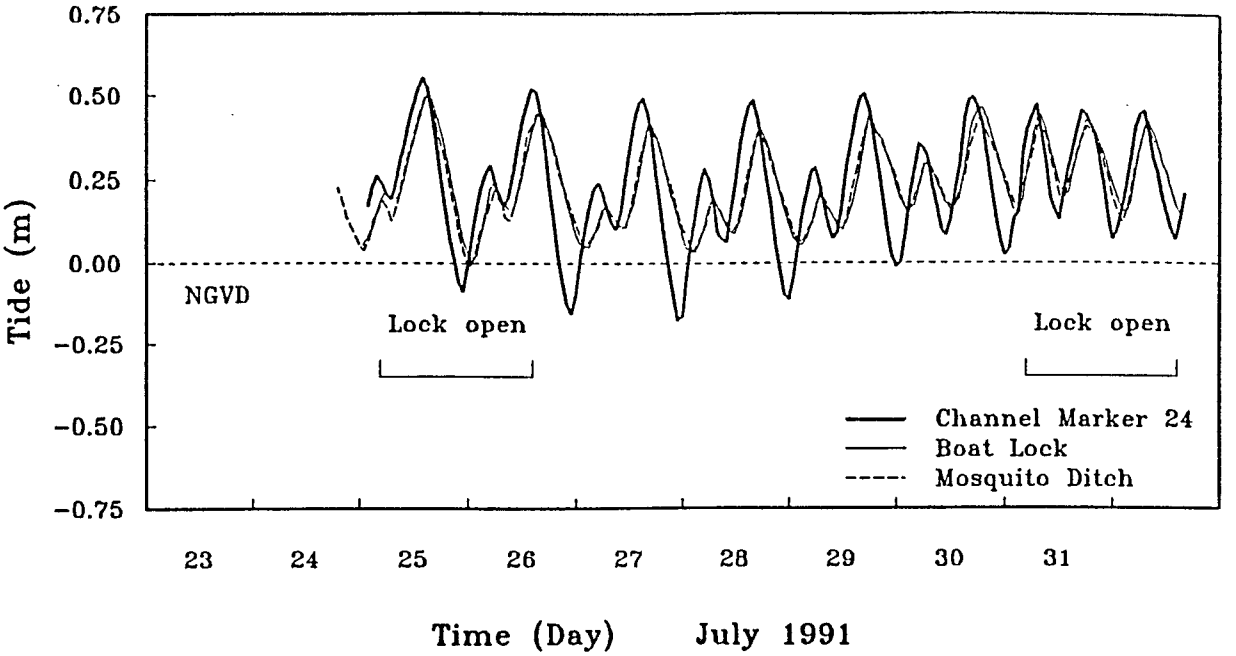

Figure 3: Tidal histories measured during the summer experiment.

and semi-diurnal. During the eight-day recording period, the diurnal component was predominant first whereas the semi-diurnal component gradually took over at the later time. The boat lock was closed most the time except during normal boat transit period and two one-day periods when the field crews conducted current measurements. These two one-day periods are marked on the same graph. The tidal ranges were larger during the time when the diurnal component dominates. The maximum tidal range at Station 7 in the eight-day measurements was in the order of 0.7 m (2.3 ft). This tidal range roughly represents the median tidal condition in this region.

It is noticed in Figure 3 that the water surface fluctuation histories measured at the mosquito ditch and at the boat lock are nearly identical for the entire record irrespective whether the lock was open or closed. The tide at Channel Marker 24 led these at the mosquito ditch and boat lock as expected so were the tidal ranges which were always larger at Channel Marker 24 location.

The current measurements taken at individual cross-sectional stations, in general, consisted of three vertical profiles, each with two to three depth levels depending upon the water depth. The areal averaged velocities at each stations are given in Figure 4. Based on these measurements the flow discharges, Q, through individual stations are computed. The results are summarized in Table 1 together with the tidal elevations at the boat lock and at Channel Marker 24 at the time the measurements were taken. Figure 5 plots the discharge against the water level difference, ΔH, between the lock and Channel Marker 24. The positive Q indicates flow up to the creek from the Charlotte Harbor and negative Q corresponds to flow downstream towards the Harbor. A number of observations are made here:

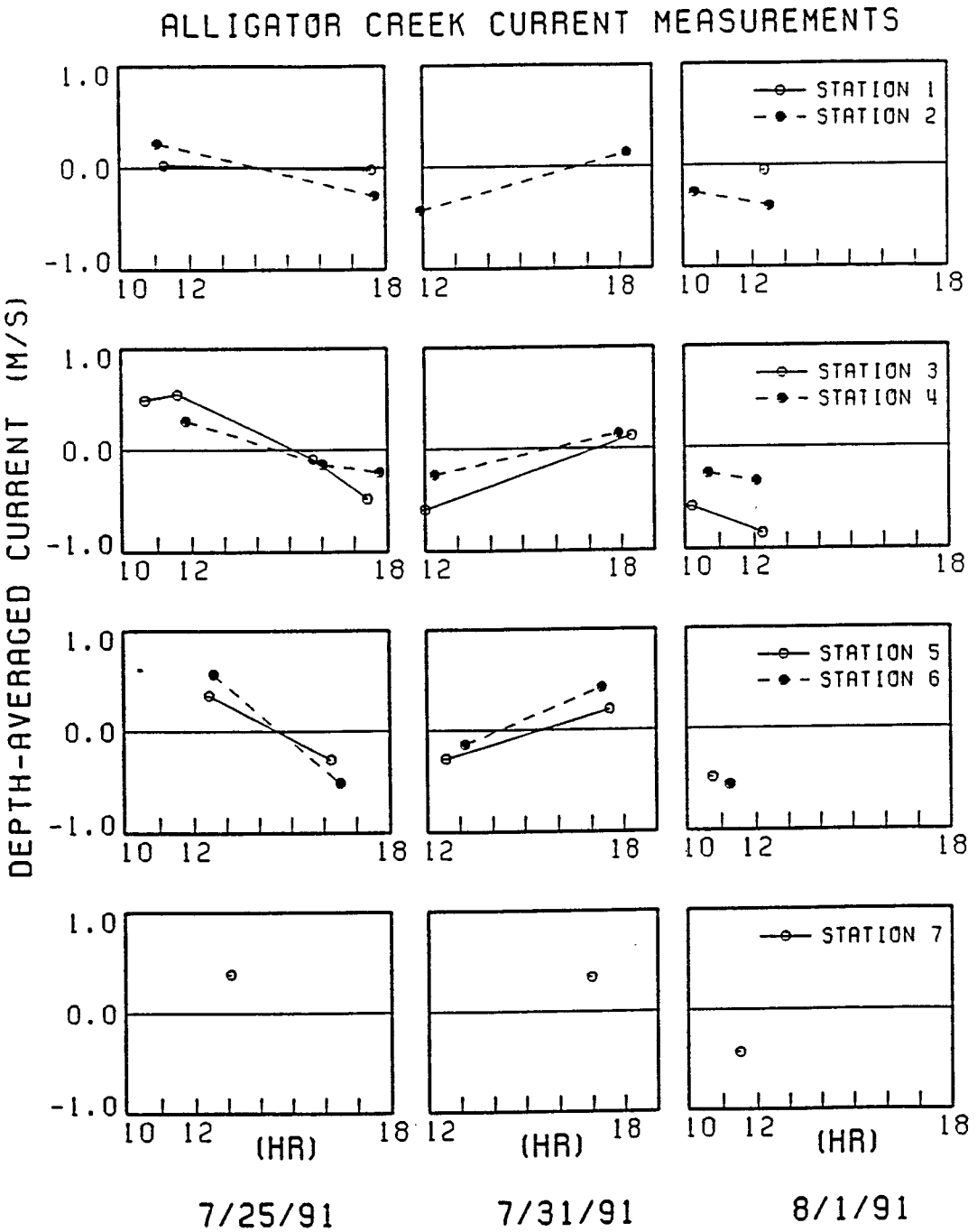

Figure 4: Depth-averaged velocities from the summer measurements.

Table 1: Measured summer discharges and water surface elevations.

Station I.D.	Date	Time	Discharge* (m^3/sec)	Tidal Elevation(m)	
				Boat Lock	Channel Marker 24
1	7/25/91	11:15	1.03	0.34	0.44
		17:36	-1.04	0.37	0.29
	8/01/91	12:22	-2.53	0.21	0.14
2	7/25/91	11:04	9.08	0.33	0.43
		17:40	-10.77	0.37	0.29
	7/31/91	11:56	-15.82	0.22	0.14
		18:13	5.28	0.41	0.44
	8/01/91	10:21	-10.10	0.32	0.25
		12:30	-14.81	0.21	0.13
3	7/25/91	10:39	7.09	0.31	0.40
		11:36	8.49	0.36	0.45
		15:45	-1.77	0.48	0.47
		17:24	-9.37	0.38	0.31
	7/31/91	12:00	-10.21	0.21	0.13
		18:20	2.12	0.41	0.43
	8/01/91	10:13	-9.01	0.32	0.26
		12:14	-12.19	0.22	0.14
4	7/25/91	11:50	22.64	0.37	0.47
		16:02	-11.98	0.46	0.44
		17:46	-22.05	0.36	0.28
	7/31/91	12:19	-22.80	0.20	0.16
		17:56	12.69	0.40	0.45
	8/01/91	10:41	-22.51	0.30	0.23
		12:04	-27.57	0.23	0.15
5	7/25/91	12:07	24.47	0.39	0.48
		16:21	-22.86	0.44	0.41
	7/31/91	12:45	-16.72	0.23	0.20
		17:44	15.08	0.40	0.45
	8/01/91	10:50	-31.05	0.29	0.22
6	7/25/91	12:36	39.12	0.41	0.50
		16:31	-36.07	0.43	0.40
	7/31/91	13:11	7.82	0.20	0.23
		17:20	27.18	0.39	0.45
	8/01/91	11:14	-35.54	0.27	0.19
7	7/25/91	13:05	45.77	0.43	0.53
		16:55	-49.83	0.41	0.36
	7/31/91	16:58	29.11	0.37	0.45
	8/01/91	11:30	-48.13	0.26	0.18

* positive (negative) value indicating the flood (ebb) condition.

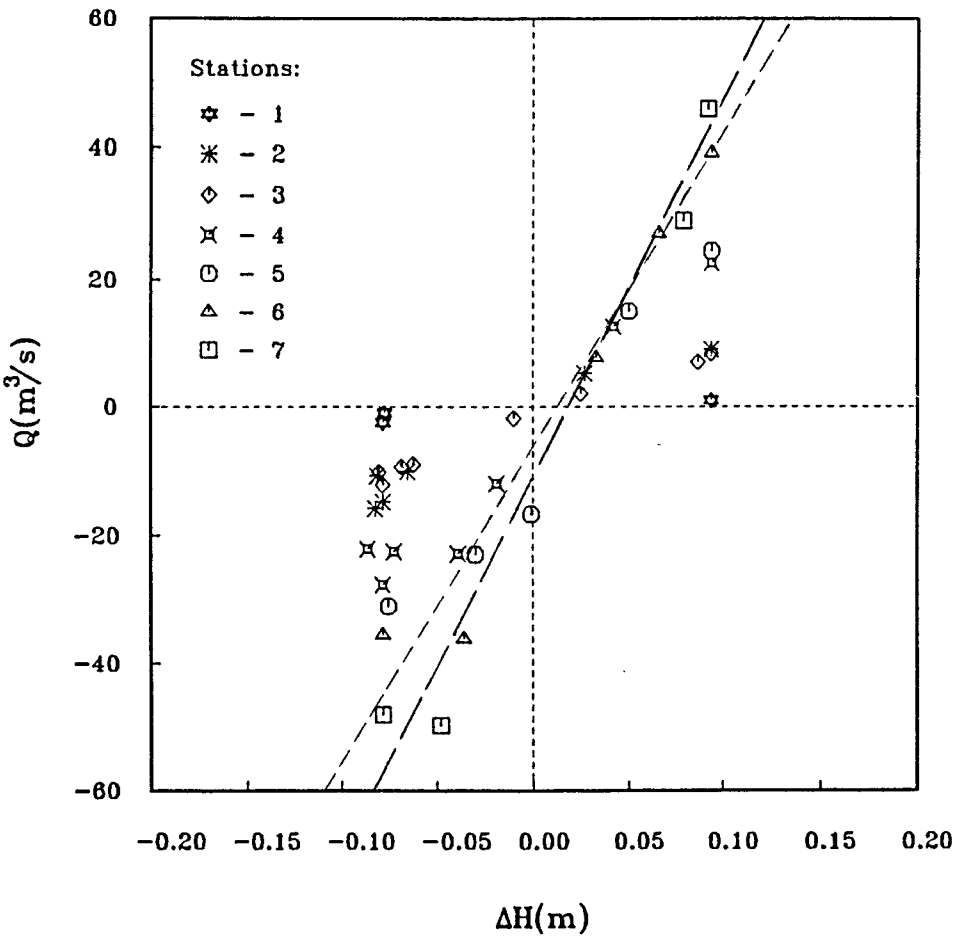

Figure 5: Plot of discharge versus head difference from the summer measurements.

1. For the same head difference, the magnitude of $+Q$ is seen to be smaller than that of $-Q$ indicating a net river discharge from upstream.

2. The measured maximum flow rate for the complete creek system was in the order of -50 m^3/s (1,750 ft^3/s). The maximum flow rate through the lock was about one-third of this value.

3. The flow through Station 1 is negligible under both flood and ebb conditions for lock open condition, which indicates that the flow collected along the northern portion of the trunk canal has other outlets. Two of these other

outlets were found. One is the narrow ditch which connects the canal and the creek just north of the lock. Another is a short, shallow opening between the canal and creek near the most northern edge of the trunk canal.

4. The flow through the lock is mainly from the south trunk when the lock is kept open. This was confirmed by tracking floating drogues through the lock section. Figures 6 and 7 show the flow patterns during flood and ebb tides, respectively. Clearly, almost all the flow through the lock is from the southern portion of the trunk canal.

5. The above observation led us to conduct a brief drogue tracking study in May, 1992 aimed at determining the flow pattern in the trunk canal south of the boat lock when the lock is kept open. It is seen from Figure 8 that the flow exchange between the southern part (South end zone) of the Section 15 and the Alligator Creek is mainly through the mosquito ditch. The flow exchange in the central portion (Central zone) of the development in mainly through the lock to the North Alligator Creek.

More detailed analysis will be presented later.

3.2 Winter Measurements

The tidal gages were put in operation just before the arrival of a spring tidal cycle. The water surface fluctuation histories at the three locations are shown in Figure 9. The nature of the tide was almost purely diurnal during the first half of the eight-day recording and then gradually turned into a mixture of diurnal and semi-diurnal. Again, like the summer measurement, the tidal ranges were larger when diurnal component dominated. Maximum tidal range measured during this period was about 1 m (3.3 ft) which was larger than the maximum tidal range observed in the summer measurement period.

The PUV gages at the lock location and at Station 6 yielded simultaneous water surface and current records as presented in Figure 10. In general, the currents are fairly well behaved and are governed mainly by the tidal elevation differences between upstream and downstream. Since the tidal differences maintain nearly constant for a significant portion of the tidal cycle, the ebb and flood conditions dominate with very short slack water time. This situation is illustrated in Figure 11 by plotting the current measured together with the tidal differences between boat lock and Channel Marker 24. The currents are modest with maximum in the order of 0.6 m/s at the lock location and of 0.4 m/s at Station 6. With these records the residue currents can also be established. The values are +0.0 m/s at the lock and +0.01 m/s towards the north at Station 6.

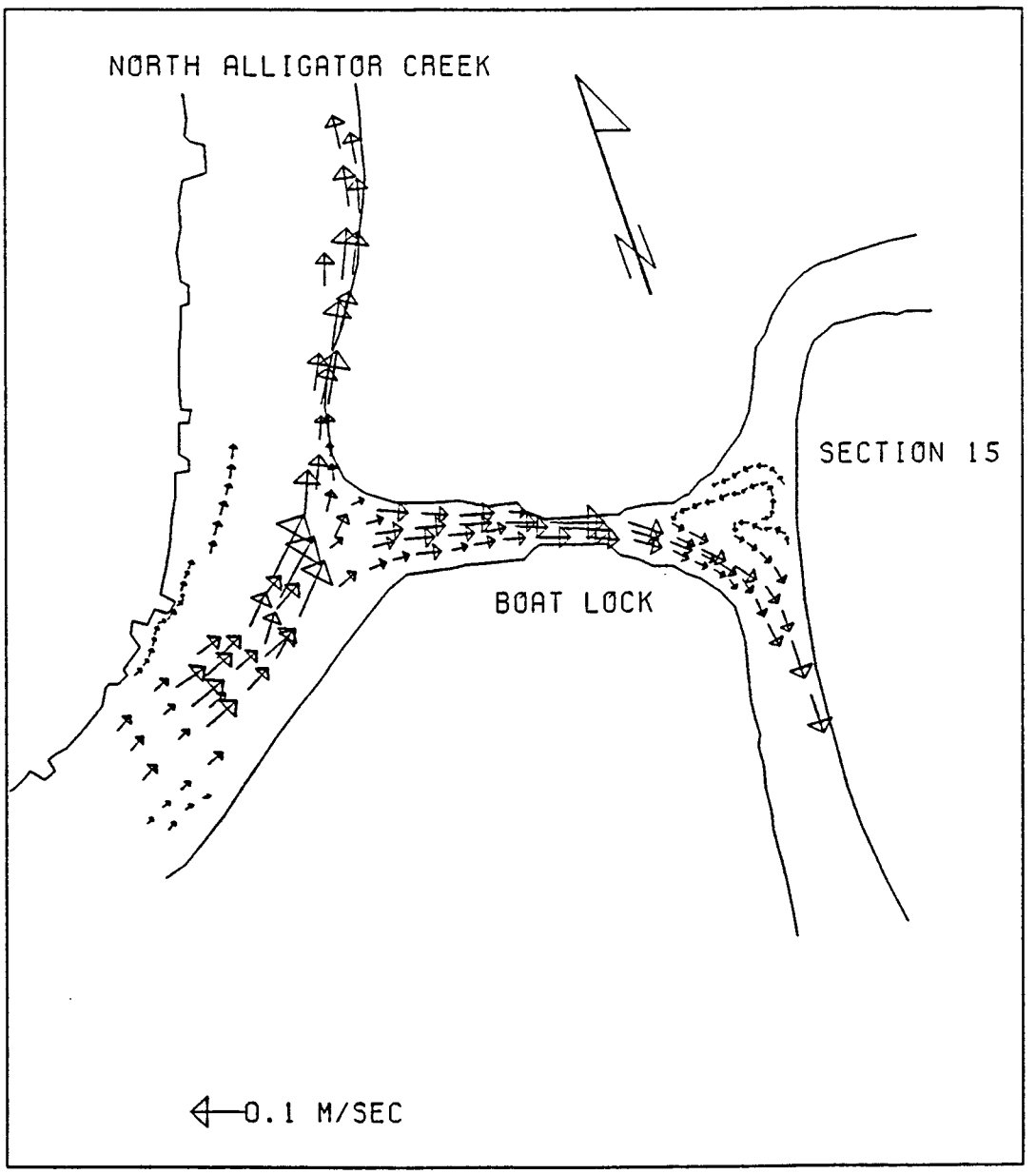

Figure 6: Flood flow pattern monitored at the boat lock.

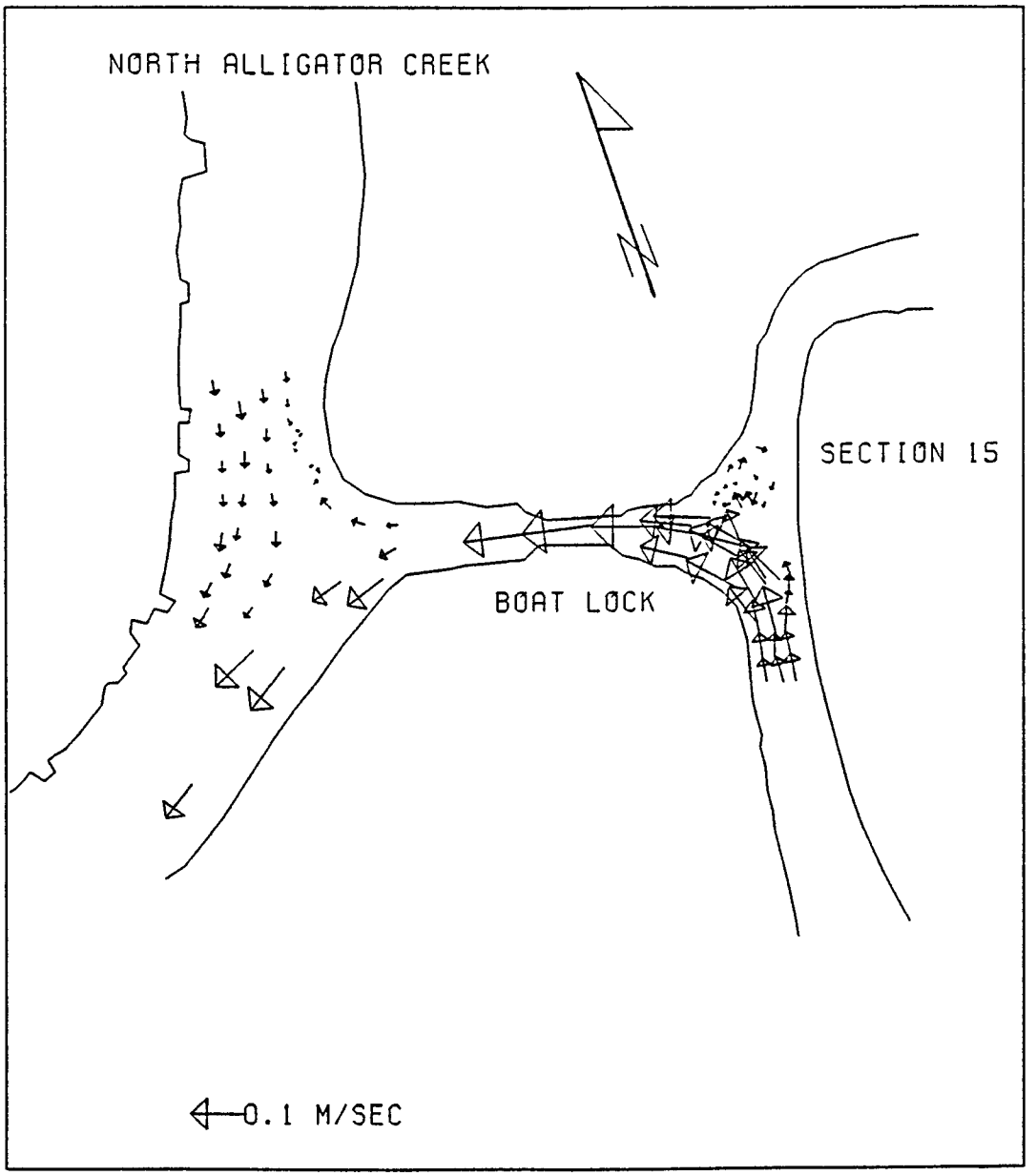

Figure 7: Ebb flow pattern monitored at the boat lock.

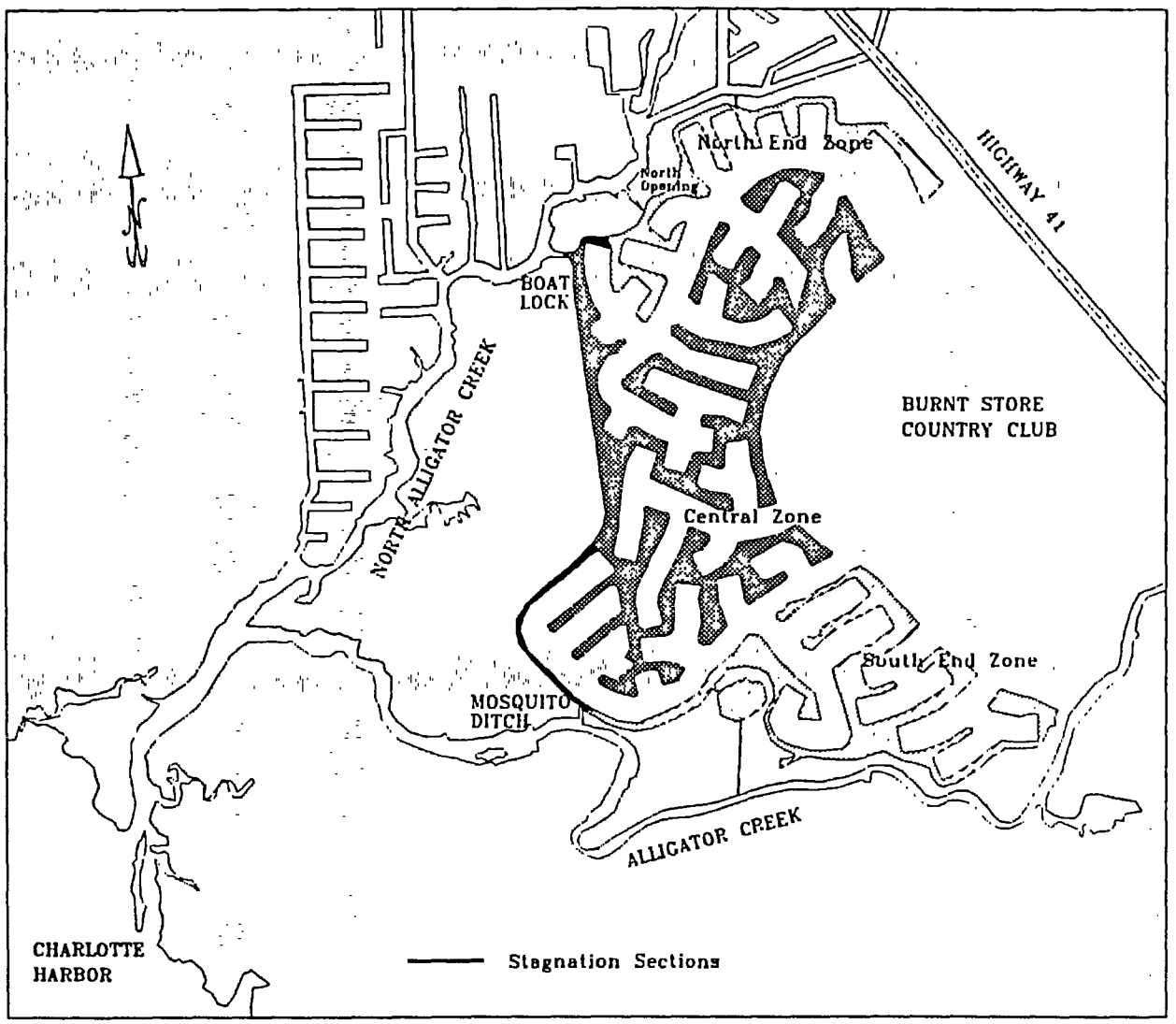

Figure 8: Flow exchange zones from a brief drogue tracking study.

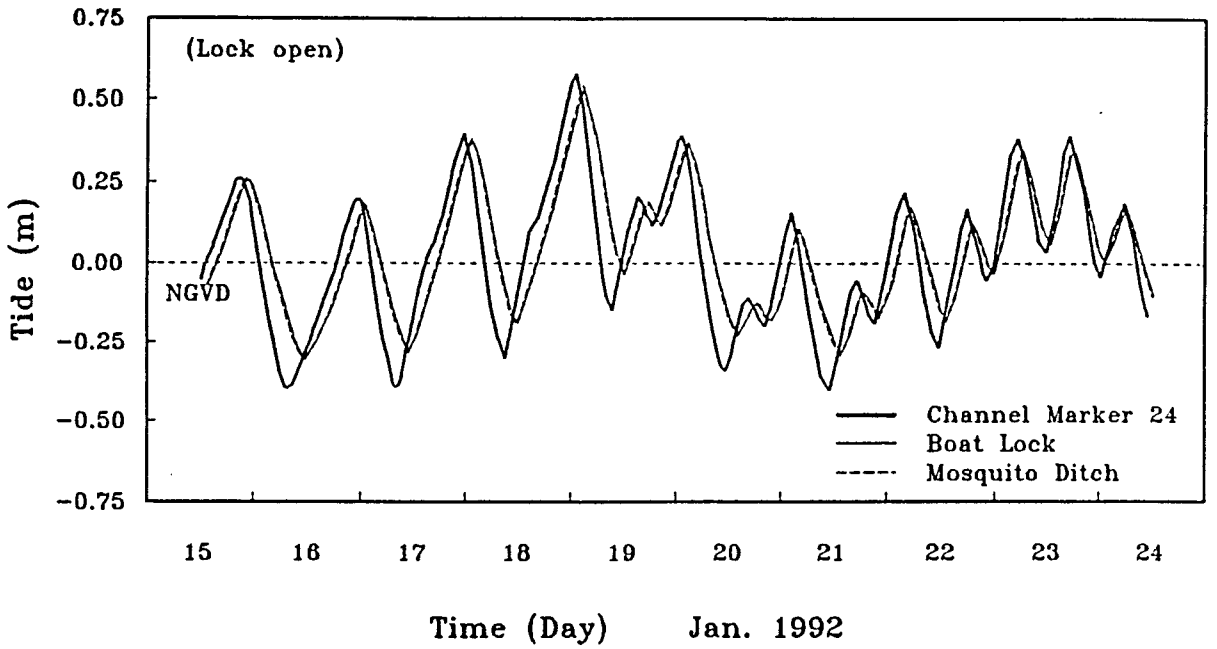

Figure 9: Tidal histories measured during the winter experiment.

The cross-sectional current measurements were again taken at the same seven stations as in the summer experiments. The areal averaged currents at the seven cross-sectional stations are shown in Figure 12. The flow discharges, Q, through the each of the seven stations are then computed. The results are listed in Table 2 together with the tidal elevations measured at the same time at the boat lock and at Channel Marker 24. The plot of discharges versus head differences is given in Figure 13. The magnitudes of the flow discharges are of the same order as the summer values. However, for the same head difference the $+Q$ and $-Q$ are nearly the same indicating negligible net creek discharge during the measurement period.

The results of the dye dispersion test together with the tides and currents recorded at the lock during the test are presented in Figure 14.

4 Numerical Modeling

A one-dimensional numerical model was developed for this study. The purpose of the model is to argument the field data for estimation of discharges at various points in the study area and to assess the dispersion characteristics at the boat lock. The computational domain and grid point system of the model are given in Figure 15. The creek and trunk channels in the computational domain is actually described by a simplified flow network in the model. The network consists

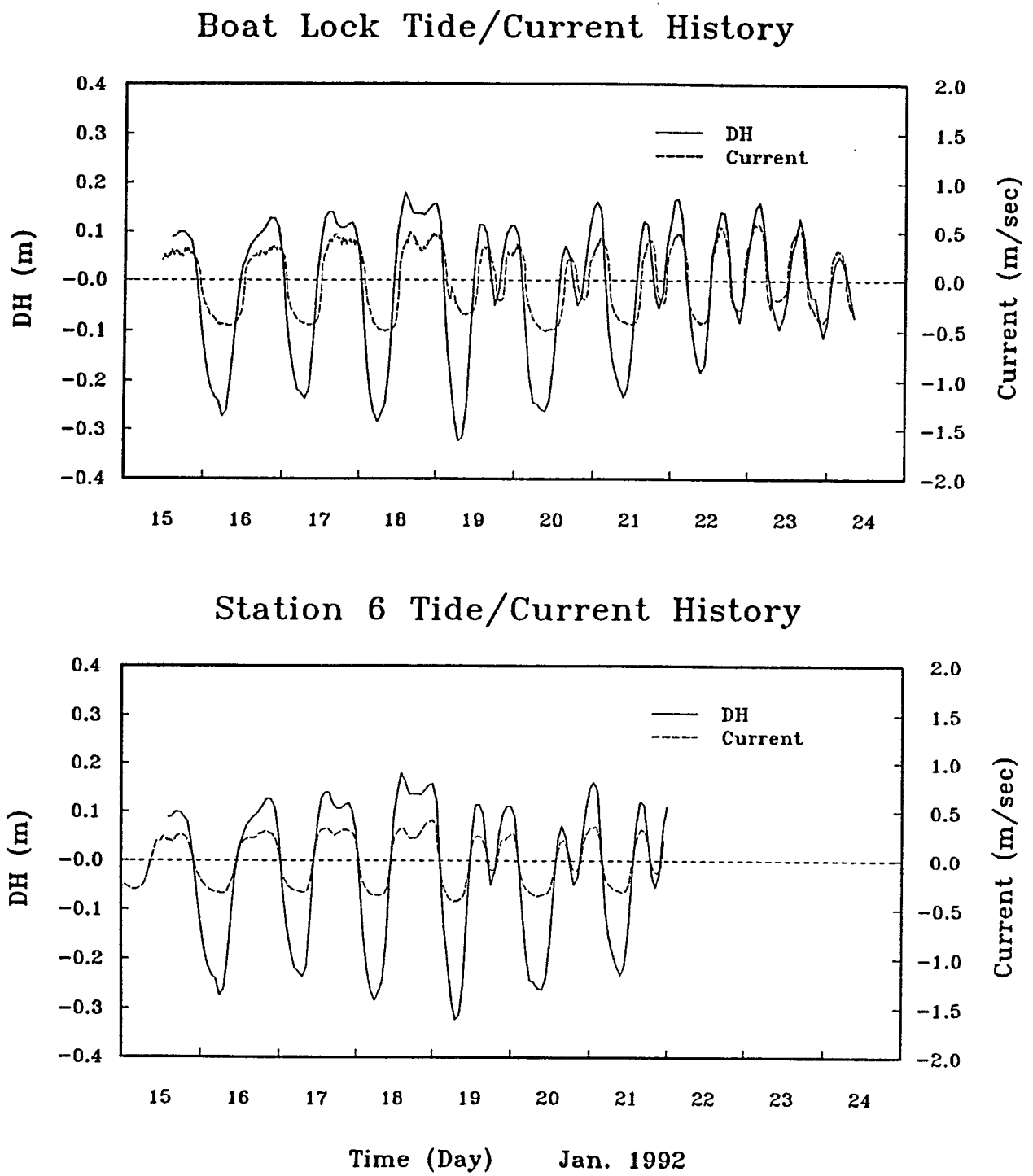

Figure 10: Water surface and current measurements at the boat lock and Station 6.

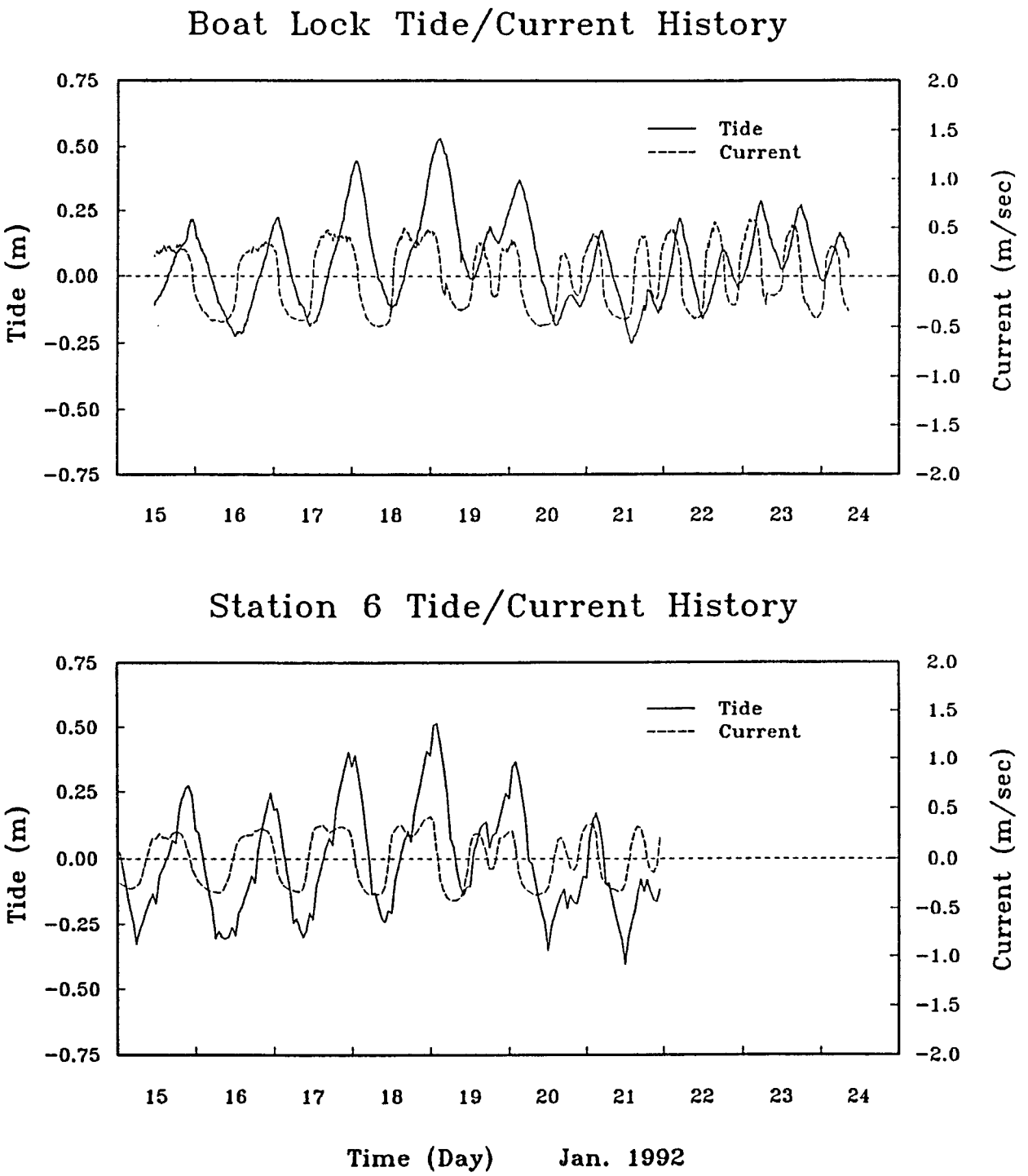

Figure 11: Plots of measured currents versus head differences.

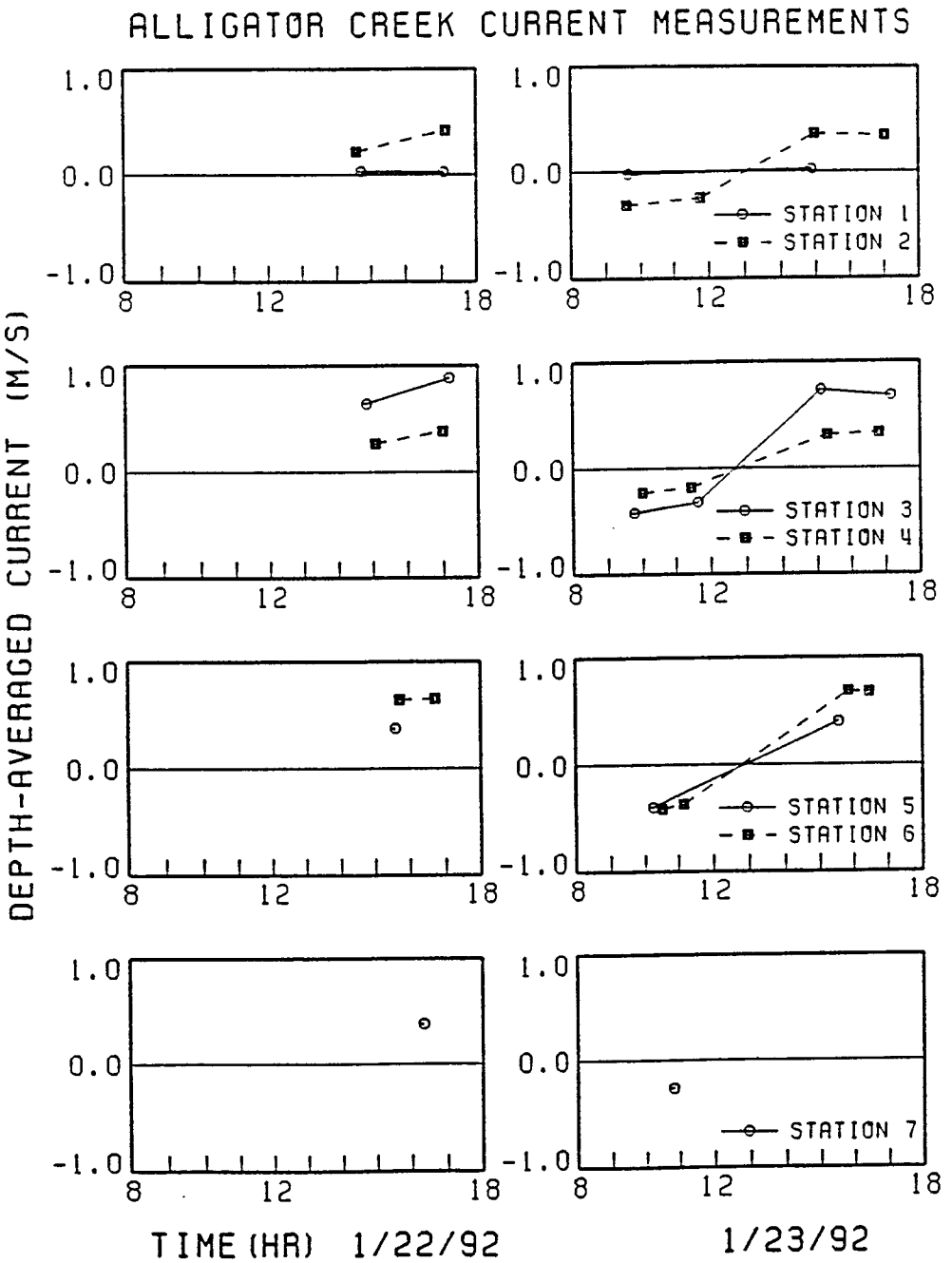

Figure 12: Depth-averaged velocities from the winter measurements.

Table 2: Measured winter discharges and water surface elevations.

Station I.D.	Date	Time	Discharge* (m^3/sec)	Tidal Elevation(m)	
				Boat Lock	Channel Marker 24
1	1/22/92	14:43	1.43	-0.11	-0.01
		17:04	1.31	0.03	0.14
	1/23/92	09:37	-0.98	0.18	0.10
2	1/22/92	14:35	7.15	-0.12	-0.02
		17:05	14.48	0.03	0.15
	1/23/92	09:35	-11.52	0.18	0.10
		11:46	-8.82	0.08	0.04
		14:57	13.28	0.19	0.27
		17:00	13.30	0.33	0.39
3	1/22/92	14:50	9.44	-0.11	-0.01
		17:11	13.64	0.04	0.15
	1/23/92	09:45	-6.81	0.17	0.09
		11:38	-5.00	0.09	0.04
		15:07	12.17	0.20	0.29
		17:10	11.87	0.33	0.39
4	1/22/92	15:04	16.85	-0.09	0.02
		17:00	27.69	0.03	0.14
	1/23/92	10:00	-22.46	0.15	0.07
		11:25	-14.75	0.09	0.04
		15:17	23.40	0.21	0.30
		16:47	24.67	0.31	0.38
5	1/22/92	15:20	25.74	-0.08	0.04
	1/23/92	10:11	-27.18	0.14	0.06
		15:32	31.08	0.23	0.32
6	1/22/92	16:41	32.34	0.01	0.13
	1/23/92	10:31	-22.25	0.12	0.06
		11:10	-19.10	0.10	0.05
		15:50	40.32	0.25	0.35
		16:26	37.61	0.29	0.37
7	1/22/92	16:19	37.69	-0.01	0.11
	1/23/92	10:49	-29.45	0.11	0.05
		16:11	38.86	0.27	0.36

* positive (negative) value indicating the flood (ebb) condition.

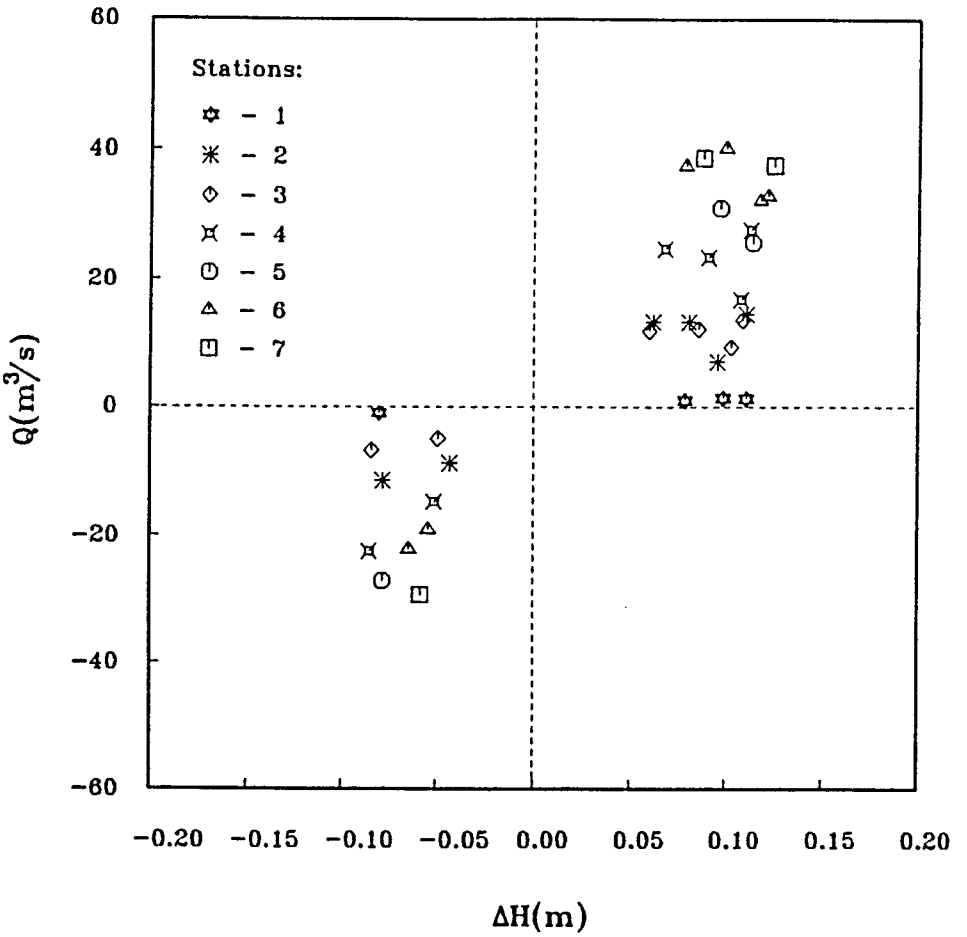

Figure 13: Plot of discharge versus head difference from the winter measurements.

of prismatic channels representing the Alligator Creek, the north branch of the Alligator Creek and the trunk canal portion in section 15. The finger canals and small tributaries are treated as storages.

A brief description of the numerical model, including governing equations as well as computational schemes, is given as follows.

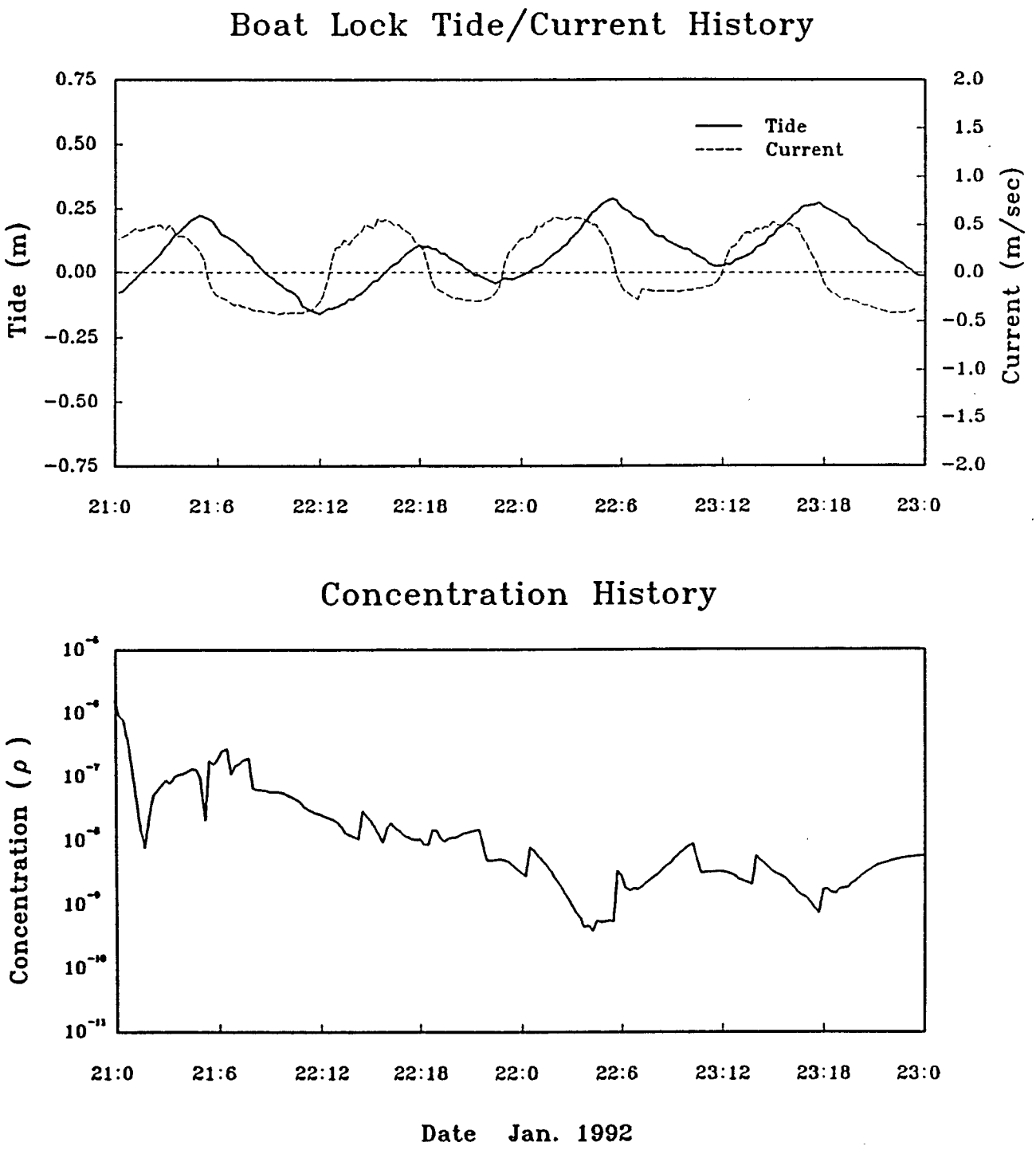

Figure 14: Plot of concentration of Rhodamine dye versus time.

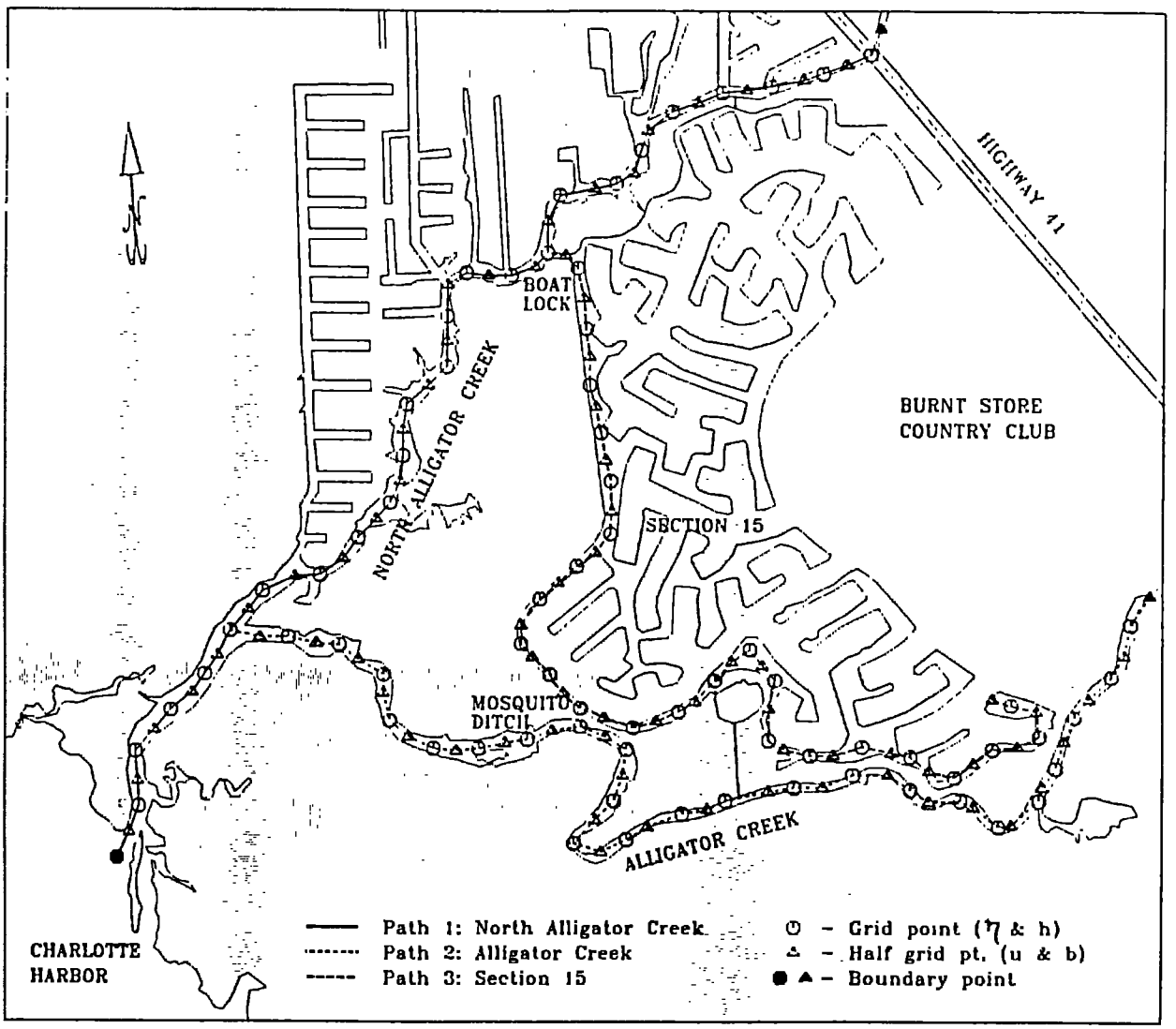

Figure 15: Area and grid point system considered in the model.

4.1 Basic Equations

The one-dimensional equations of continuity, momentum and transport-diffusion are used as basic equations of the model to predict surface elevation, current velocity and concentration of any dissolved matter [1].

$$b\frac{\partial \eta}{\partial t} + \frac{\partial Q}{\partial x} - q = 0 \tag{1}$$

$$\frac{\partial Q}{\partial t} + \frac{\partial uQ}{\partial x} + gA\frac{\partial \eta}{\partial x} + gb\frac{|u|u}{C^2} = 0 \tag{2}$$

$$\frac{\partial}{\partial t}(Ac) + \frac{\partial}{\partial x}(Qc) - qc_l - \frac{\partial}{\partial x}(AK\frac{\partial c}{\partial x}) = 0 \tag{3}$$

where, η =surface elevation,
Q=flow rate,
u=velocity,
q =lateral influx,
g =gravity acceleration,
b =channel width,
A=channel area,
C=Chezy coefficient,
c =concentration (c_l=concentration of lateral influx),
K=dispersion coefficient.

The Chezy coefficient, C, is related to the Darcy-Weisbach resistance coefficient, f, by the formula

$$C = \sqrt{\frac{8g}{f}}$$

4.2 Numerical Methods

Equations (1) and (2) can be expressed on the staggered grid system by finite difference as

$$\frac{\eta^{n+1} - \eta^{n-1}}{2\Delta t} + \frac{1}{\bar{b}}\frac{(Ub)_i - (Ub)_{i-1}}{\Delta x} - \frac{q_s + q_b}{\bar{b}} = 0 \tag{4}$$

$$\frac{U^{n+1} - U^{n-1}}{2\Delta t} + \frac{(uUb)_{i+1} - (uUb)_{i-1}}{2b_i\Delta x} + g\bar{h}\frac{\eta_{i+1} - \eta_i}{\Delta x} + \frac{f|u^n|U^{n+1}}{8\bar{h}} = 0 \tag{5}$$

where U is the depth integrated velocity, and $\bar{b}$ and $\bar{h}$ are the average width and depth, respectively; the subscripts s and b refer to storage and branch, respectively. Referring to Figure 15 the surface elevation, concentration and water depth are

defined at grid point whereas the flux and width are given at half-grid point. The storages and branches are connected at grid points, their elevations are assumed to be the same there. Assuming that the surface variation in the storage areas is instantaneous, Eq.(5) can be rewritten as

$$\frac{\eta^{n+1}-\eta^{n-1}}{2\Delta t}+\frac{1}{\bar{b}}\frac{(Ub)_i-(Ub)_{i-1}}{\Delta x}-\frac{1}{\bar{b}}\left(\frac{\frac{S(\eta^{n+1}-\eta^{n-1})}{2\Delta t}+(Ub)_b}{\Delta x}\right)=0 \qquad (6)$$

where S is the surface area of storage. The above finite difference equations, Eqs.(6) and (7) are solved by implicit finite difference scheme. The convective term in Eq.(6) is assumed to be negligible. There are two kinds of boundary conditions as shown in Figure 15. One is the open boundary condition at sea end which is given as the recorded tidal history, and the other is the upstream boundary conditions which are specified as the influxes from rivers.

Equation (3) is solved by a Lagrangian formulation which takes the following term

$$\frac{Dc}{Dt}=K\frac{\partial^2 c}{\partial x^2} \qquad (7)$$

where K is assumed to be constant. Equation (8) is solved in two fractional steps at each time step: (i) by the transport of concentration elements due to convection, and (ii) by the random walk displacement of the same elements due to dispersion [2]. The convection operator allows the displacement of each element by the velocity computed from the hydrodynamic model. Once the velocity is obtained, it is easy to have

$$x_j(t+\delta t)=x_j+u(x_j)\delta t$$

for jth element by using a first-order difference formula.

The dispersion operator with an impulse as initial condition has a solution which is the probability density function of a Gaussian distribution with zero mean and a variance $2K\delta t$. Therefore, the dispersive transport of concentration elements is simulated by adding to their convective motion and additional random walk displacement drawn from a Gaussian distribution with zero mean and a variance $2K\delta t$. The total transport is obtained by adding the two fractional displacements.

$$x_j(t+\delta t)=x_j+u(x_j)\delta t+\eta_x \qquad (8)$$

where the last term in the right hand side is for the random walk in the x (longitudinal) direction.

The open boundary condition at sea end is assumed to be satisfied by a complete absorption without reflection. The upstream boundary conditions are satisfied by mirror-image method.

4.3 Calibration of Hydrodynamic Model

The hydrodynamic model requires the determination of one empirical coefficient, namely, the Chezy coefficient, C, or it equivalent, the Darcy-Weisbach friction coefficient, f. This was accomplished by adjusting the numerically simulated water surface and current time series to match those of the measured ones. Based upon the criterion of the best overall agreement the optimum value of the friction coefficient was determined to be f= 0.04. Figures 16 and 17 show the comparisons of the computed and measured time series of surface elevation and currents, respectively, based on f=0.04.

4.4 Estimation of Dispersion Coefficient

The longitudinal dispersion coefficient, K, used in the transport model was determined by comparing the simulated concentration variations with that measured at the boat lock (Figure 18). The optimum value of K was determined to be about 0.8 m^2/s for the trunk canal. This value appears to be reasonable for channels of narrow width but could be too small in the creek. Nevertheless, the K value is kept constant in the numerical simulation.

5 Analysis

5.1 Flow and Discharges

The main purpose of this study is to determine the flow rate through the lock and whether the closure of the lock in the summer months will effectively contain the pollutant within the canal network in the Section 15. Flow analysis was performed for the following conditions:

a. Flow under summer condition.

b. Flow under winter condition.

a. Flow Under Summer Condition

Based upon the field data it is clear that the entire flow network under consideration is tidal dominated. The contribution of stream flow from upland during the summer measurement period was estimated to be about 10 m^3/s, of which 65%

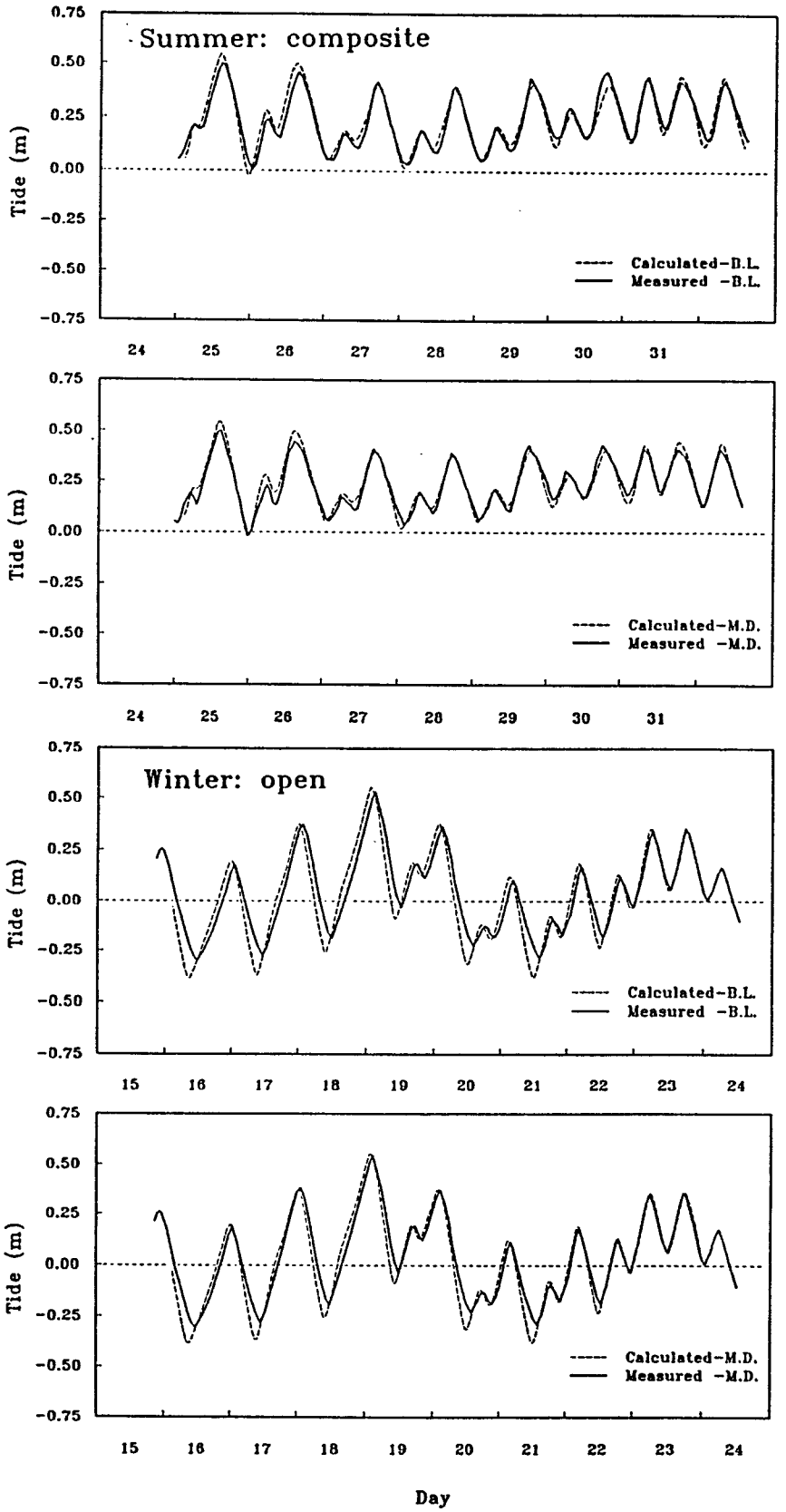

Figure 16: Comparison of computed and measured surface elevations.

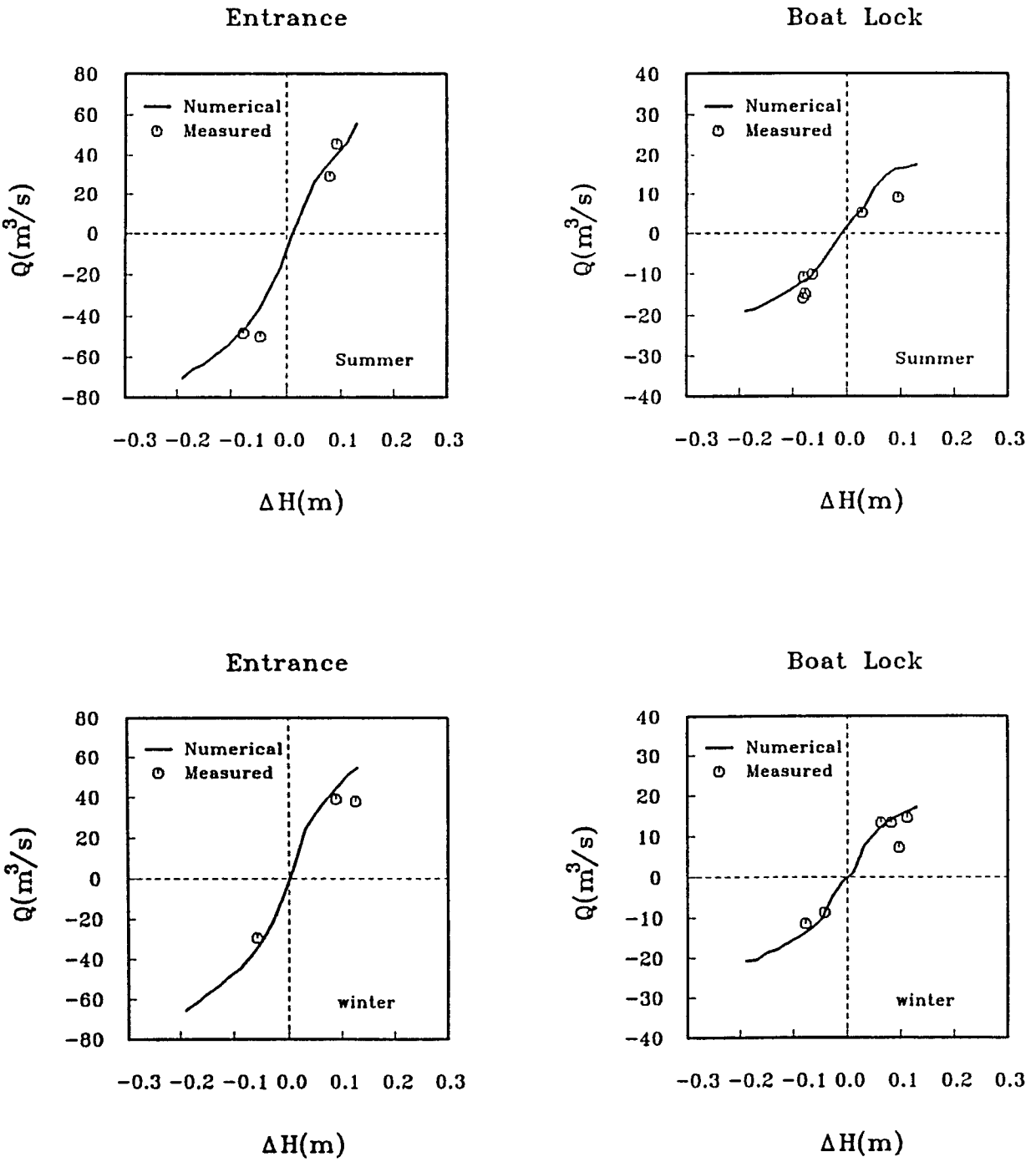

Figure 17: Comparison of computed and measured flow currents.

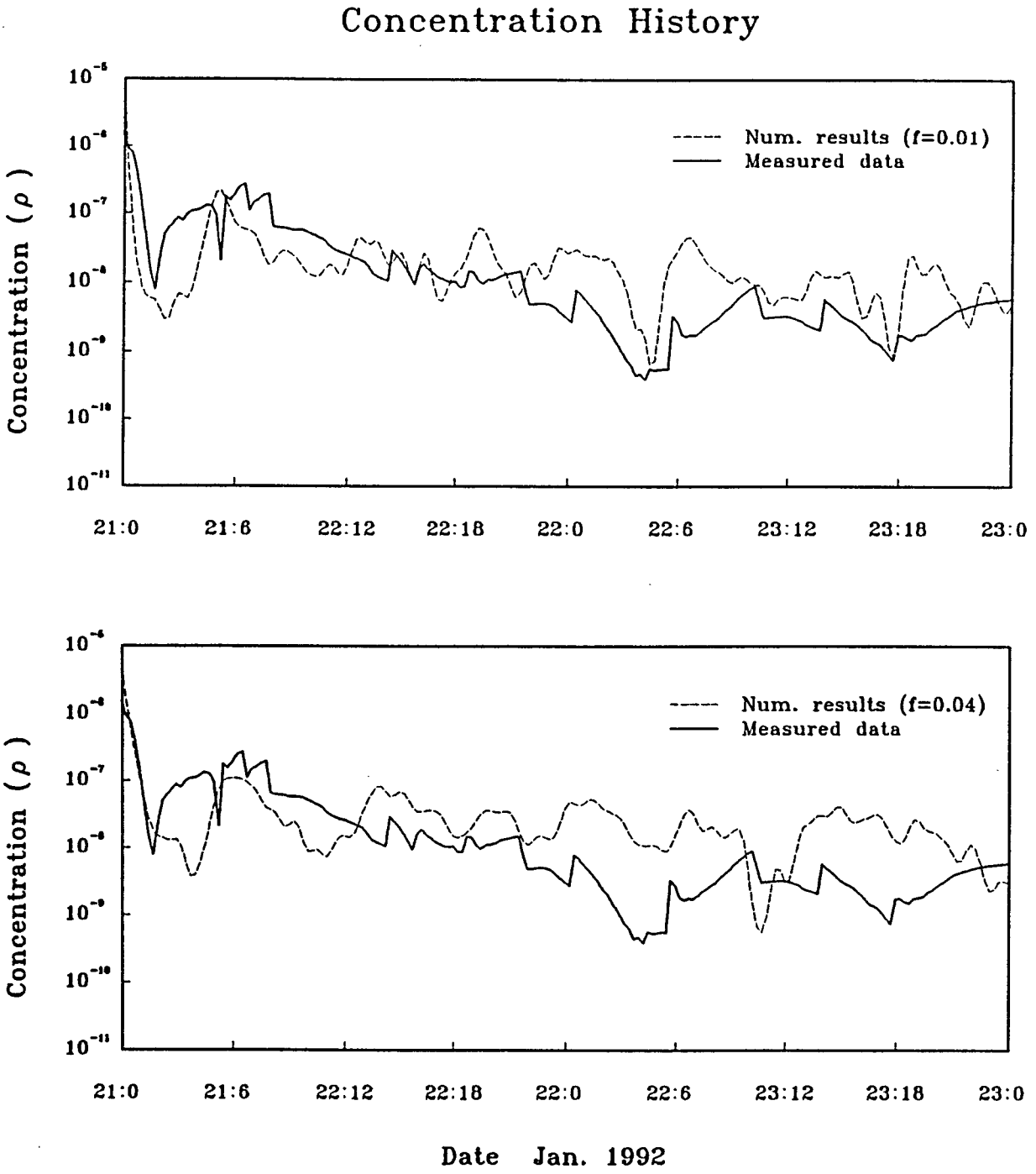

Figure 18: Comparison of computed and measured concentrations.

was from the north branch of the Alligator Creek and the remaining 35% from the main creek. These values were obtained by a simple interpretation scheme explained here.

From the flow discharge data obtained from the July, 1991 measurement one can see that the discharge at Station 7 represents the total contribution from the Alligator Creek and its north branch. If the flow is completely tidal induced, i.e., if the stream flow is zero, the time averaged flow rate (over an integral number of tidal cycles) should be equal to zero. If the stream flow is non zero, the residue represents the net stream flow. Since we do not have time averaged flow rate data, a straight line is fitted onto the Q–ΔH graph for Station 7 (Figure 5). The intersect at the ordinate approximates the net stream flow rate. This intersect is approximately equal to -10 m^3/s which represents the net stream flow. If this straight line is shifted upward by the amount of 10 m^3/s, it will pass through the origin and the condition of zero tidal induced net flow is satisfied.

The net stream flow from the north branch is obtained in a similar manner by fitting a straight line on the Q-ΔH graph (Figure 5) through the discharge data at Station 6 and the intersect with the ordinate is approximately 6.5 m^3/s which represents the net stream flow from the north branch. The difference between the above two quantities of 3.5 m^3/s is the net discharge from the Alligator Creek.

Based on the field data (Table 1), the maximum discharges measured during ebb were around -50 m^3/s at Station 7, -36 m^3/s at Station 6, and -12 m^3/s at the boat lock. The corresponding maxima during flood were 46, 40, and 9 m^3/s, respectively. Since these values were based on a very limited number of measurements, they might not be representative of the actual condition. To establish the flow conditions that are more representative of this region, the numerical model was utilized to simulate the discharge using tidal history at Station 7 as input.

The first simulation is for the lock-open condition using the eight-day recorded tidal history as input. The simulated discharge time series is shown in Figure 19 together with tidal elevation histories at Station 7, boat lock and mosquito ditch. The measured data are also plotted for comparison. Since tidal action here is a mixture of diurnal and semi-diurnal, the flows are modulated. This modulation is seen more pronounced at Station 7 than at other locations. During the period where the tide contains a mixture of diurnal and semi-diurnal components the peak ebb flow is much smaller in the semi-diurnal cycle. The peak flood flow, on the other hand, is not affected. Therefore, from Figure 19 there appears to have more peaks in flood cycles than in ebb cycles during the eight-day measurement period. If the minor peaks is neglected in the ebb cycles a representative value of peak ebb discharge can be estimated to be around -64 m^3/s at Station 7. Similarly, a representative value of peak flood at Station 7 is determined to be around +44 m^3/s. The corresponding representative peak ebb and flood values at Station 6 are -30 and +22 m^3/s, and at boat lock are -17 and +19 m^3/s, respectively.

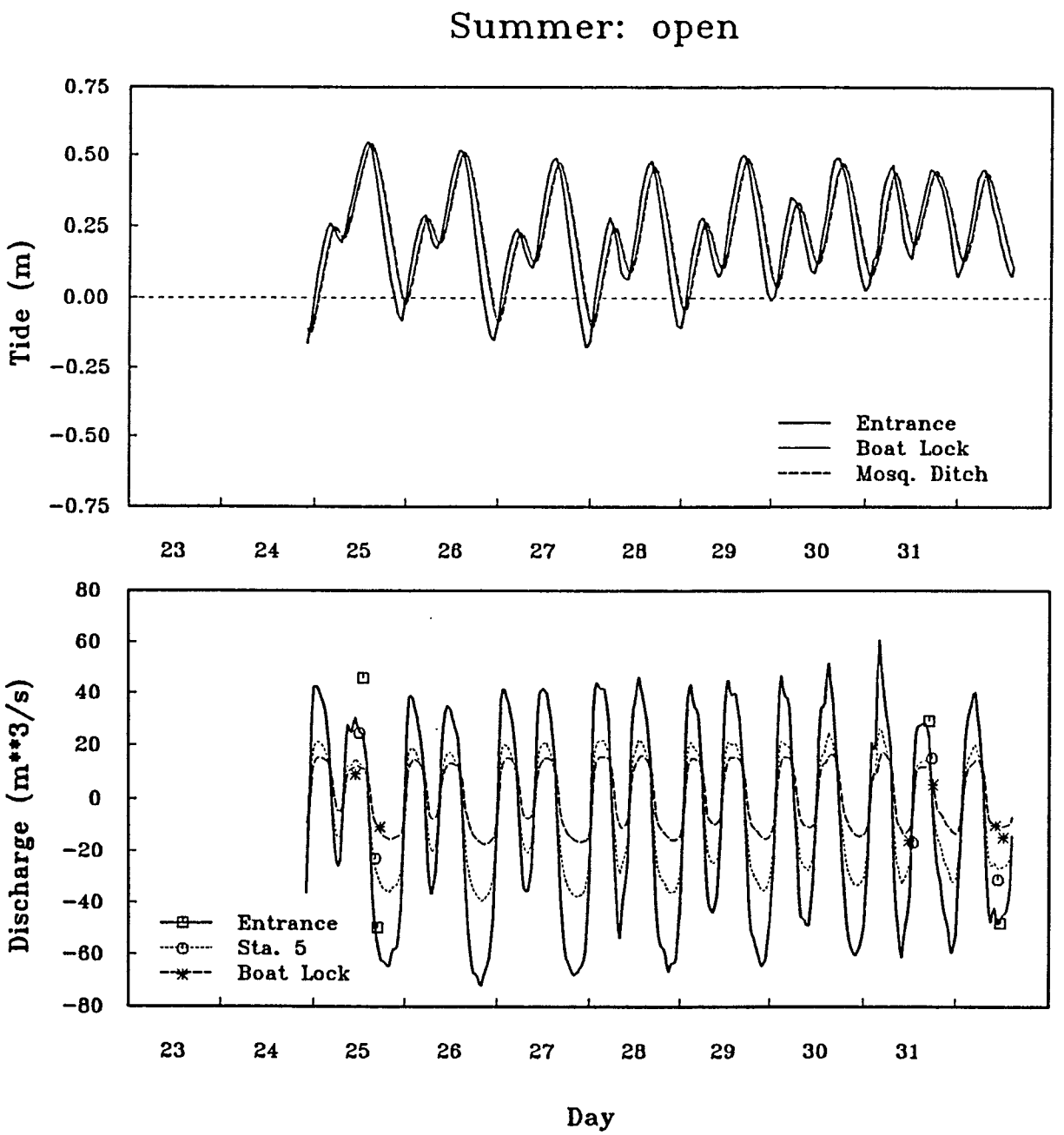

Figure 19: Simulation of discharges for the lock-open condition.

Therefore, under peak ebb condition, the flow through the lock contributes to about 32% of the tidal induced flow. Under peak flood condition, on the other hand about 35% of the tidal flow enters Section 15 through the boat lock. The difference, of course, is due to the net stream flow which is always directed towards downstream.

In addition to the peak flow values, the simulated discharge time series can be integrated to obtain the time averaged quantities. Depending upon the nature of the integrands, a number of different quantities can be established:

1. Average flood flow rate:

$$\bar{Q}_f = \frac{1}{T_f}\int_0^{T_f} q_f \mathrm{d}t$$

2. Average ebb flow rate:

$$\bar{Q}_e = \frac{1}{T_e}\int_0^{T_e} q_e \mathrm{d}t$$

3. Average gross flow rate:

$$\bar{Q}_g = \frac{1}{T_e + T_f}\int_0^{T_e+T_f} |q_e| + |g_f| \mathrm{d}t$$

4. Average net flow rate:

$$\bar{Q}_n = \frac{1}{T_e + T_f}\int_0^{T_e+T_f} (q_e + q_f) \mathrm{d}t$$

where q is the instantaneous flow rate; T is the period of recording. The subscripts e and f refer to ebb and flood, respectively. The values of the first three quantities are pretty close, with $\bar{Q}_g$ falling in between $\bar{Q}_f$ and $\bar{Q}_e$.

Figure 20 plots the flow vectors for the average flood flow rate under summer condition with the boat lock open and Figure 21 plots the average ebb flow rate under the same condition. These plots provide us with a visual display on the flow pattern as well as the magnitudes of the flow rate. Under flood condition, the simulation shows that flow enters the main channel from Charlotte Harbor, then, splits into two at the junction with bulk of the flow directing into the north branch of the Alligator Creek. The flow enters the boat lock and flows southwards with diminishing velocity and discharge. In the north branch beyond the boat lock the averaged flow is always opposite to the flood direction due to stronger net stream flow. The flood water in the Alligator Creek then enters Section 15 through the mosquito ditch and flows eastwards; the strength is much less than that through the boat lock. The stretch of canal just north of mosquito ditch to the junction at San Lorenzo Dr. is stagnant. Under ebb condition, the flows basically just reverse the directions. The strength is increased in the Alligator Creek and its

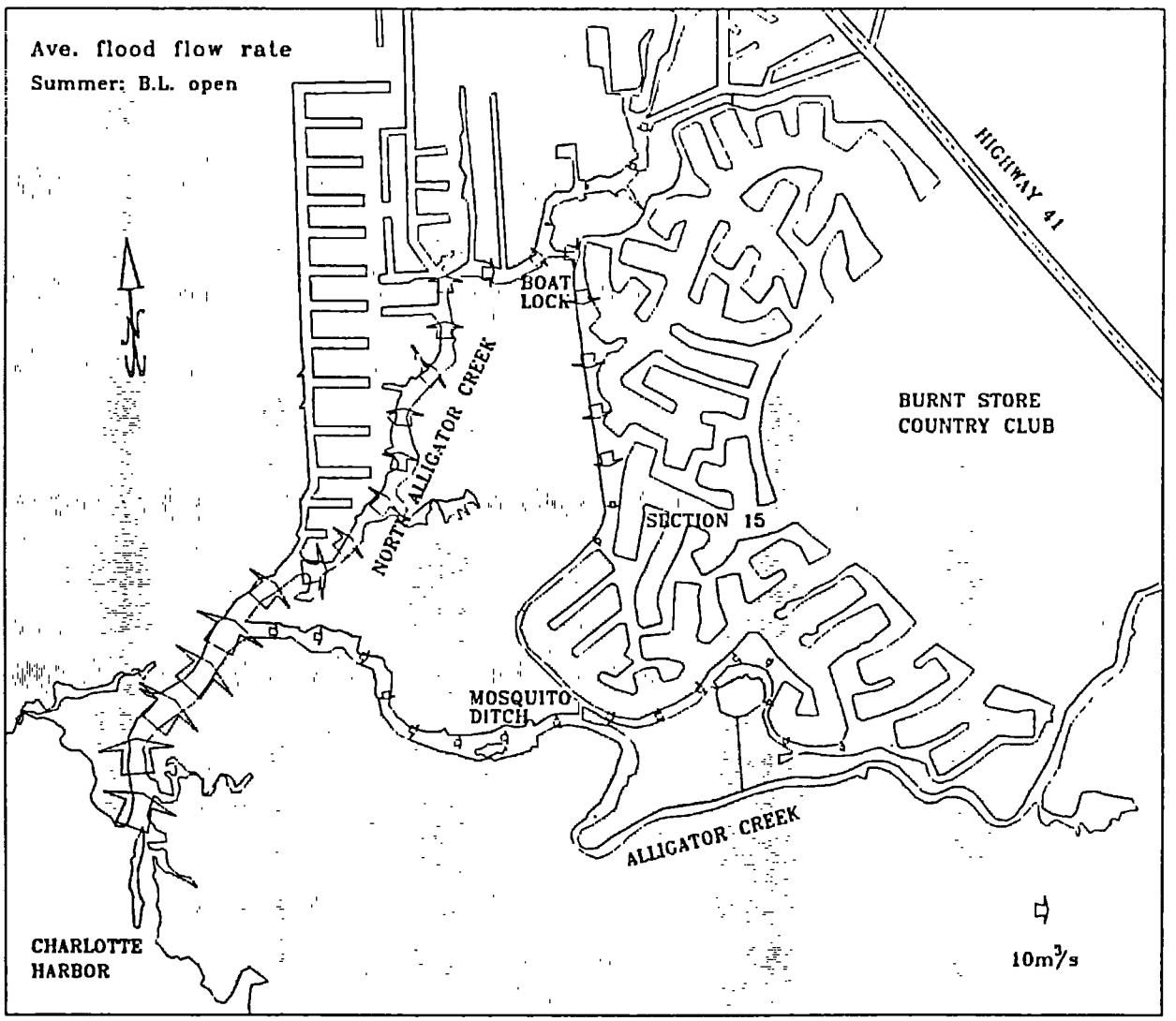

Figure 20: Flow vectors of average flood flow under summer condition.

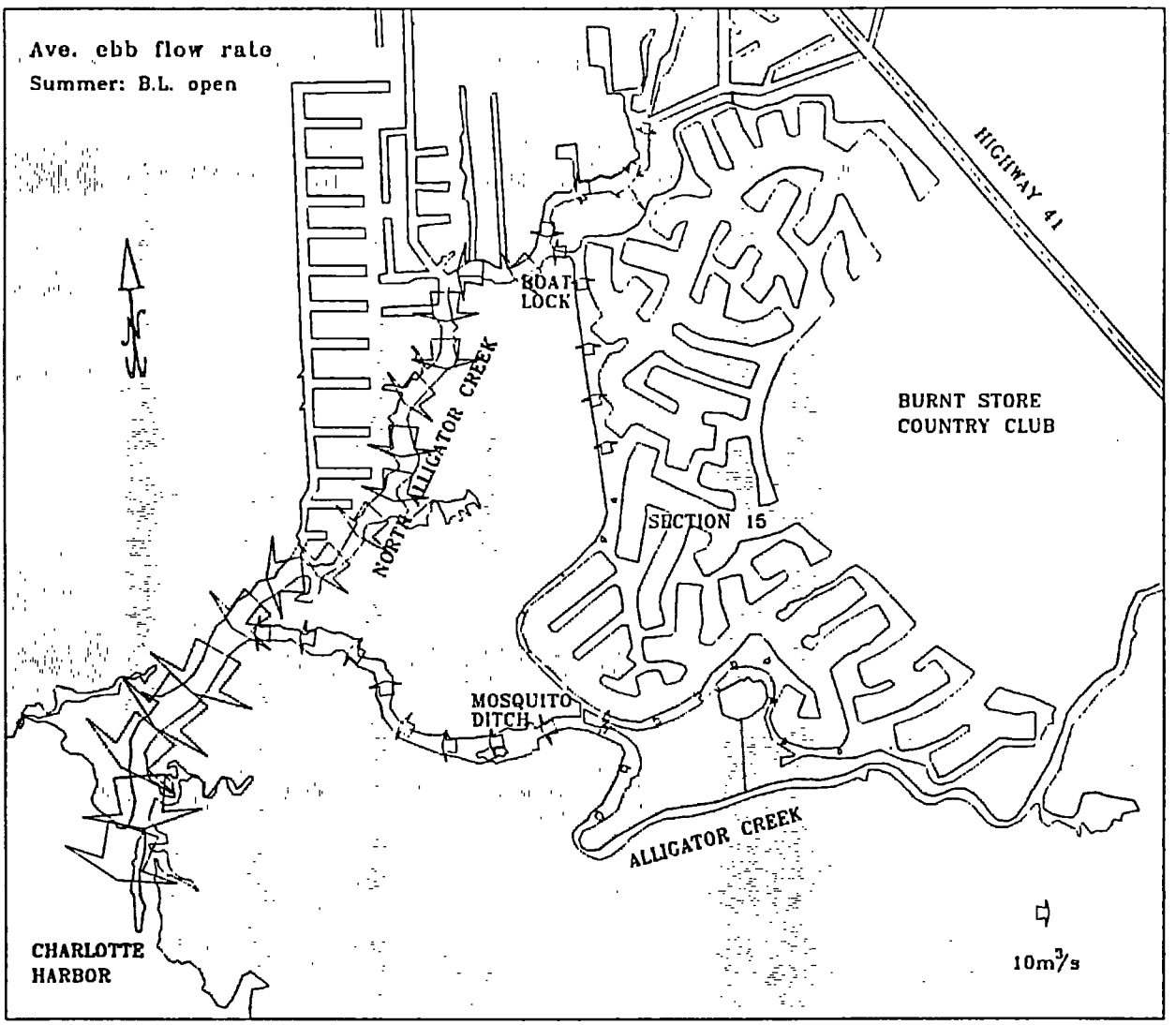

Figure 21: Flow vectors of average ebb flow under summer condition.

north branch because the net stream discharge. However, in the canal, the ebb strength is less than the flood strength. This is evidently due to the fact that portion of the stream flow in the north branch is diverted through the boat lock into the canal system. This flow is towards south, thus, aid in flood and oppose to ebb. The stagnation zone identified in the flood condition remains.

To further identify the flow contributions from various branching points, a non-dimensional plot of the gross flow rate relative to the gross rate near the mouth of the channel ($Q_{g,7}$) is produced. The plot is given in Figure 22(a)(b)(c), which show the ratios of gross flow rate, Q_g to that of $Q_{g,7}$, along three computational courses at various points. The gross flow rate as discussed earlier can be viewed as the weighted average over flood and ebb cycles. Figure 22(a) shows the change along the north branch of the Alligator Creek with the origin set at Station 7; Figure 22(b) plots the change along the Alligator Creek with the origin at the junction of the Alligator Creek and its north branch; Figure 22(c) plots the change along the south trunk of the canal beginning at the boat lock. These flow paths and the control points marked in the above figures are shown schematically in Figure 23. It is seen that the flow rate at various locations can be determined. For instance, along the trunk canal (path 3) the averaged gross flow rate through the boat lock (point I), is seen to be about 33% of the total discharge; the difference between J and K, or about 18%, represents the exchange through that part of the canal network through junction J and so on. The flows through the mosquito ditch and the north opening are seen to be about 17% and 5%, respectively. Therefore, the exchange from the combined lock, mosquito ditch and north opening equals to 55%.

The time-averaged net flow rate pattern is shown graphically in Figure 24. Clearly, part of the stream flow in the north branch diverts through the boat lock and returns to the Alligator Creek through the mosquito ditch. The strength of this branching flow is seen to be rather weak.

One of the main purposes of this study is to define the effect of lock closure versus lock opening. Therefore, the second simulation is for lock-closure condition using the measured 8-day tidal record as input. Since the lock is not completely water tight, a 85% closure is used allowing for the leakage through the bottom and the sides. Figure 25 shows the computed time series of the tides and flow rates. From here, the peak flood and ebb discharges at Station 7 are then identified as around -52 and +34 m^3/s, respectively. By comparing with the values of the lock-open condition (-65 and +45 m^3/s), the peak flow rate is reduced by about 20% during ebb and 24% during flood.

The flow patterns are also altered somewhat in Section 15. Figures 26 and 27 show the average flood and ebb patterns for the lock-closed situation. During flood, water enters the canal through the assumed 15% lock opening. This flow is joined in by the stream flow apparently diverted into the trunk canal through

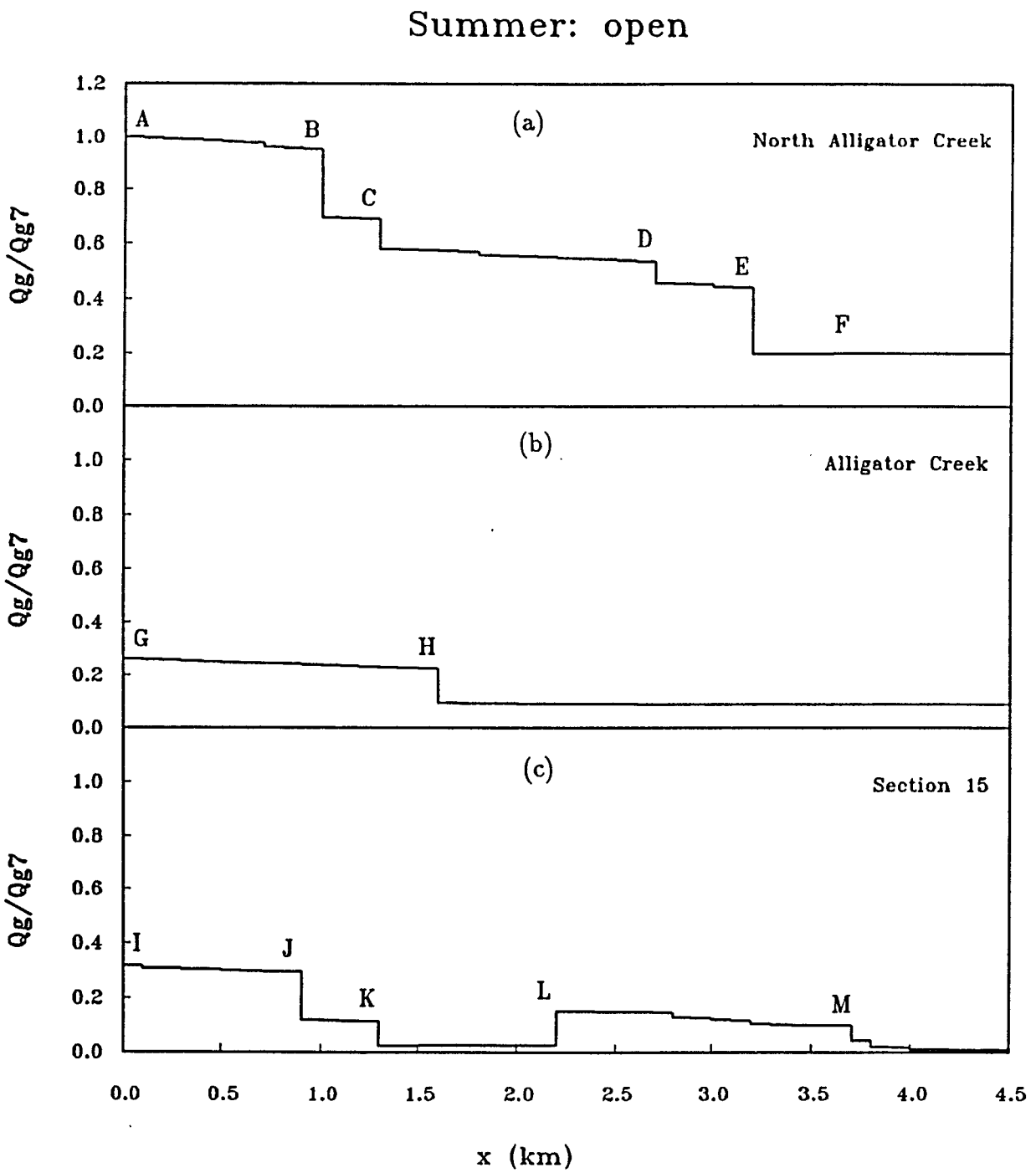

Figure 22: Non-dimensional plot of Q_g under lock-open (summer) condition.

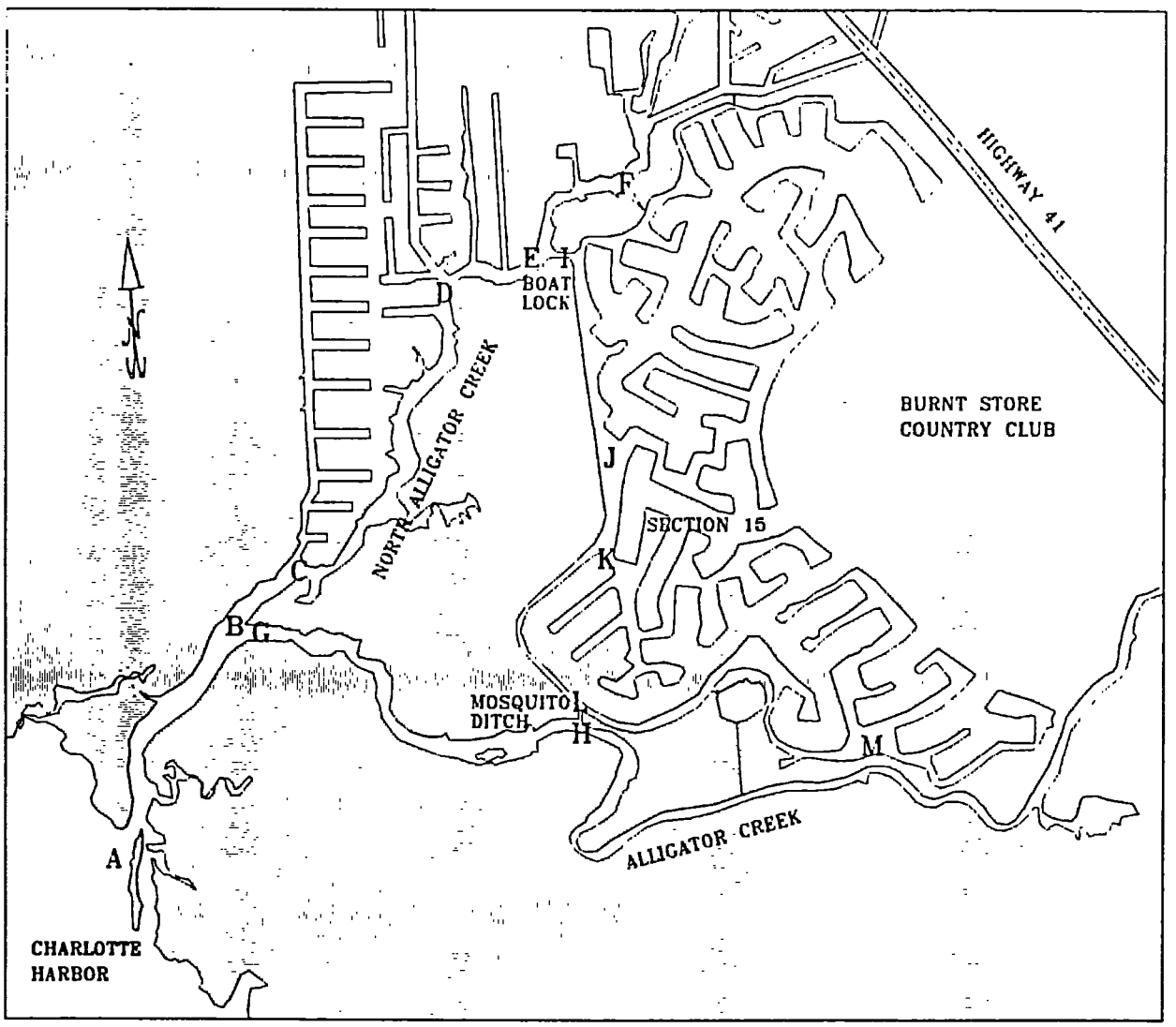

Figure 23: Location of control points (A to M) for flow rate computations.

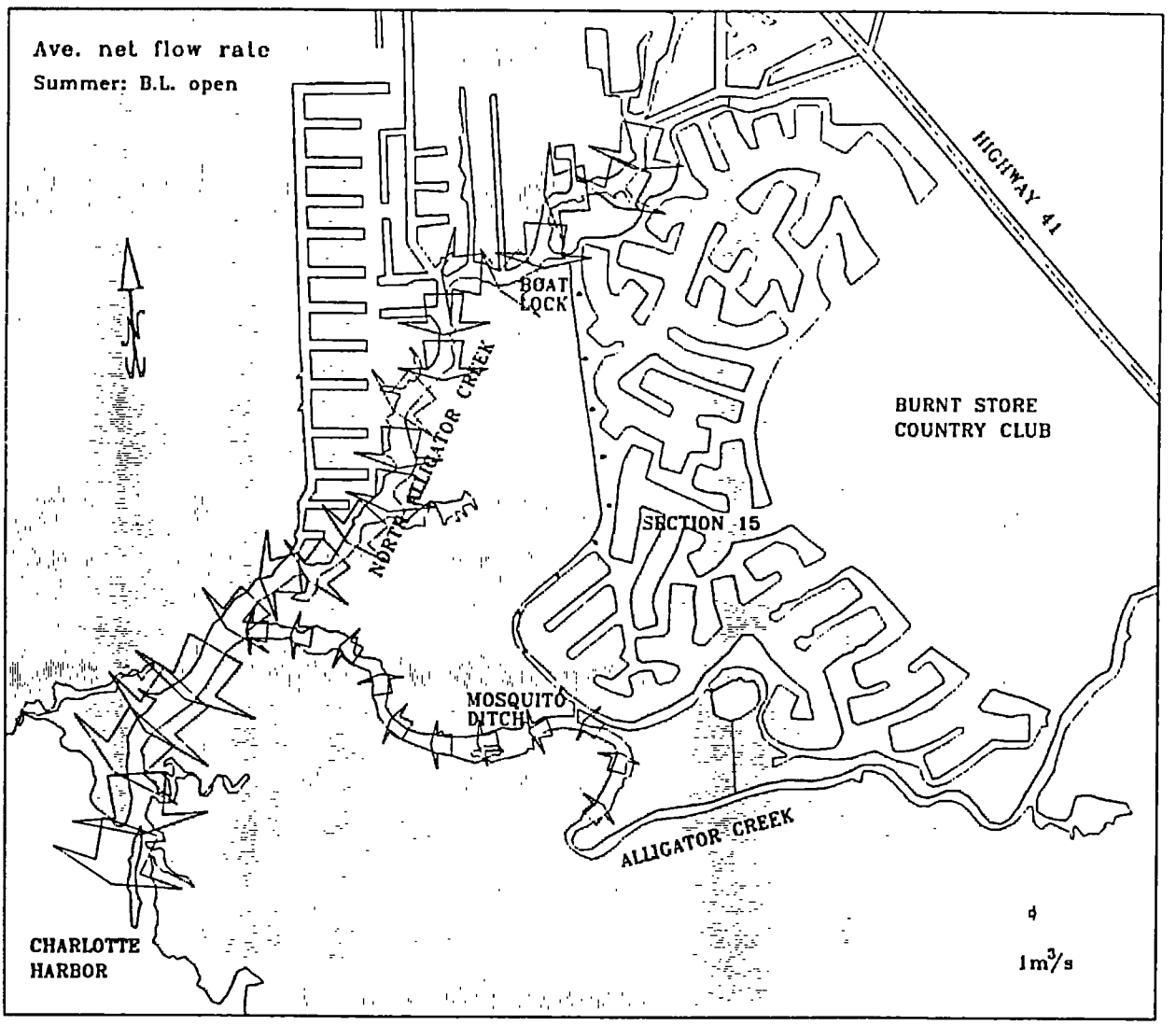

Figure 24: Time-averaged net flow pattern under lock-open (summer) condition.

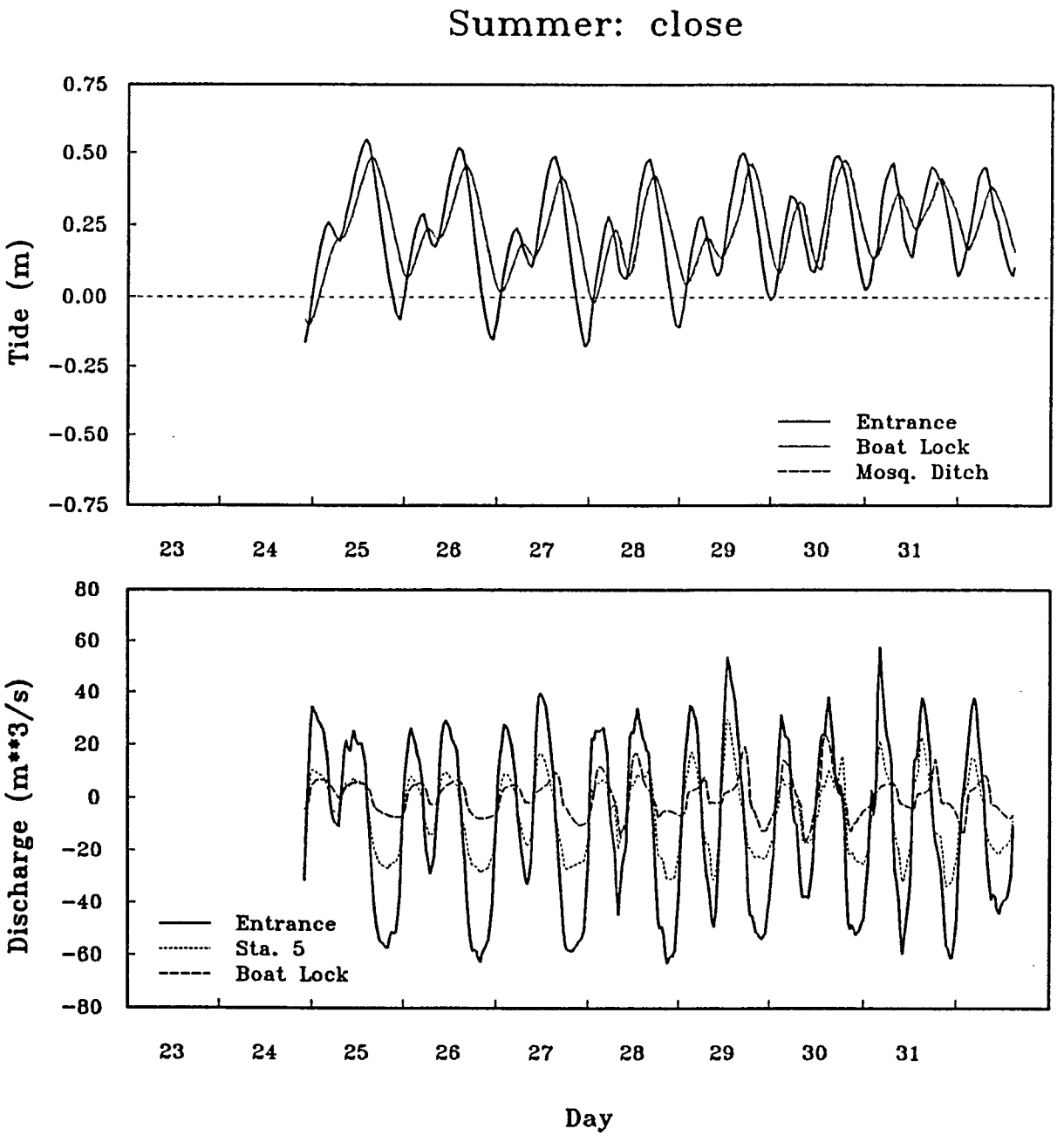

Figure 25: Computed tides and currents under the lock-closed (summer) condition.

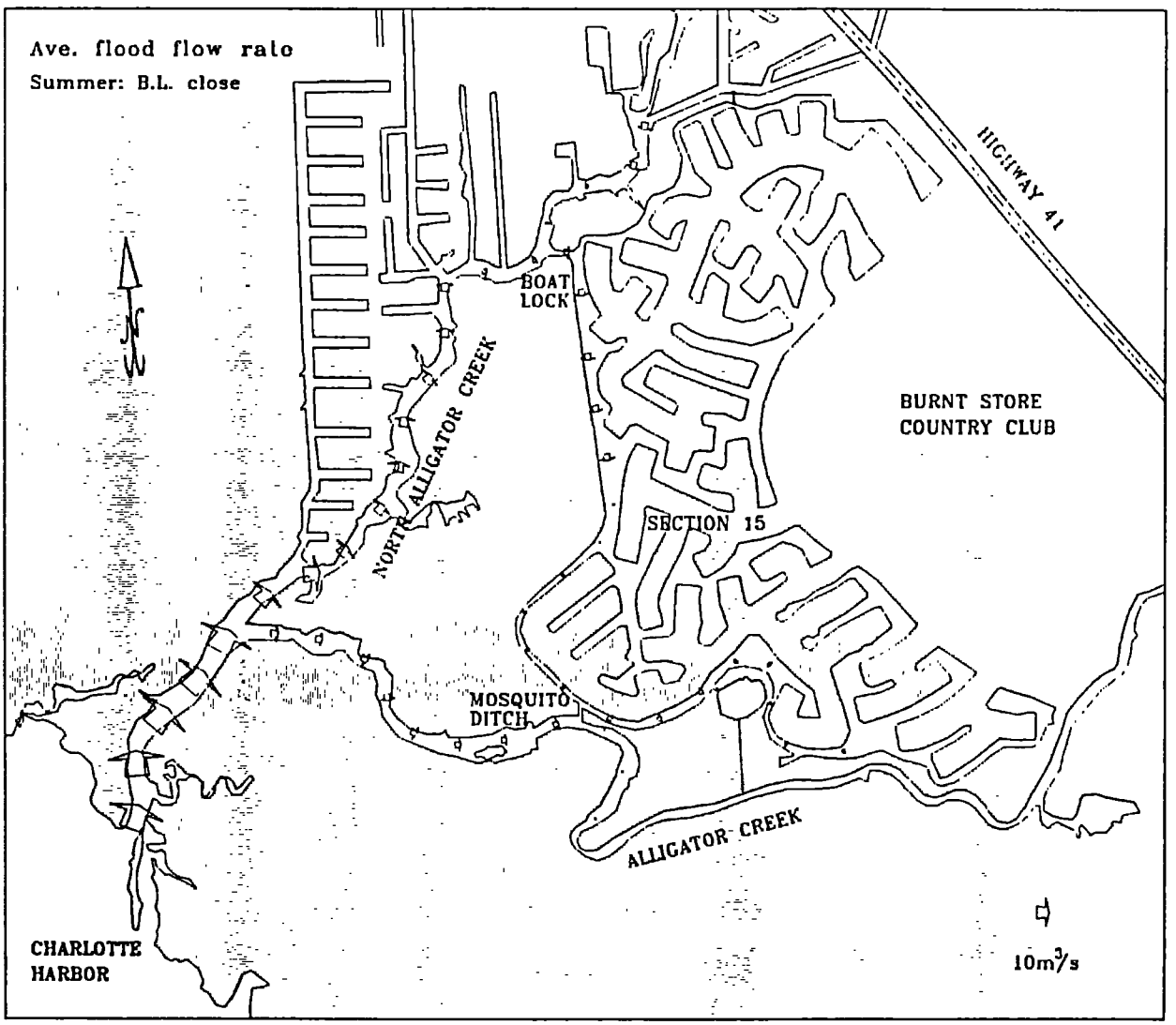

Figure 26: Time-averaged flood flow pattern under lock-closed (summer) condition.

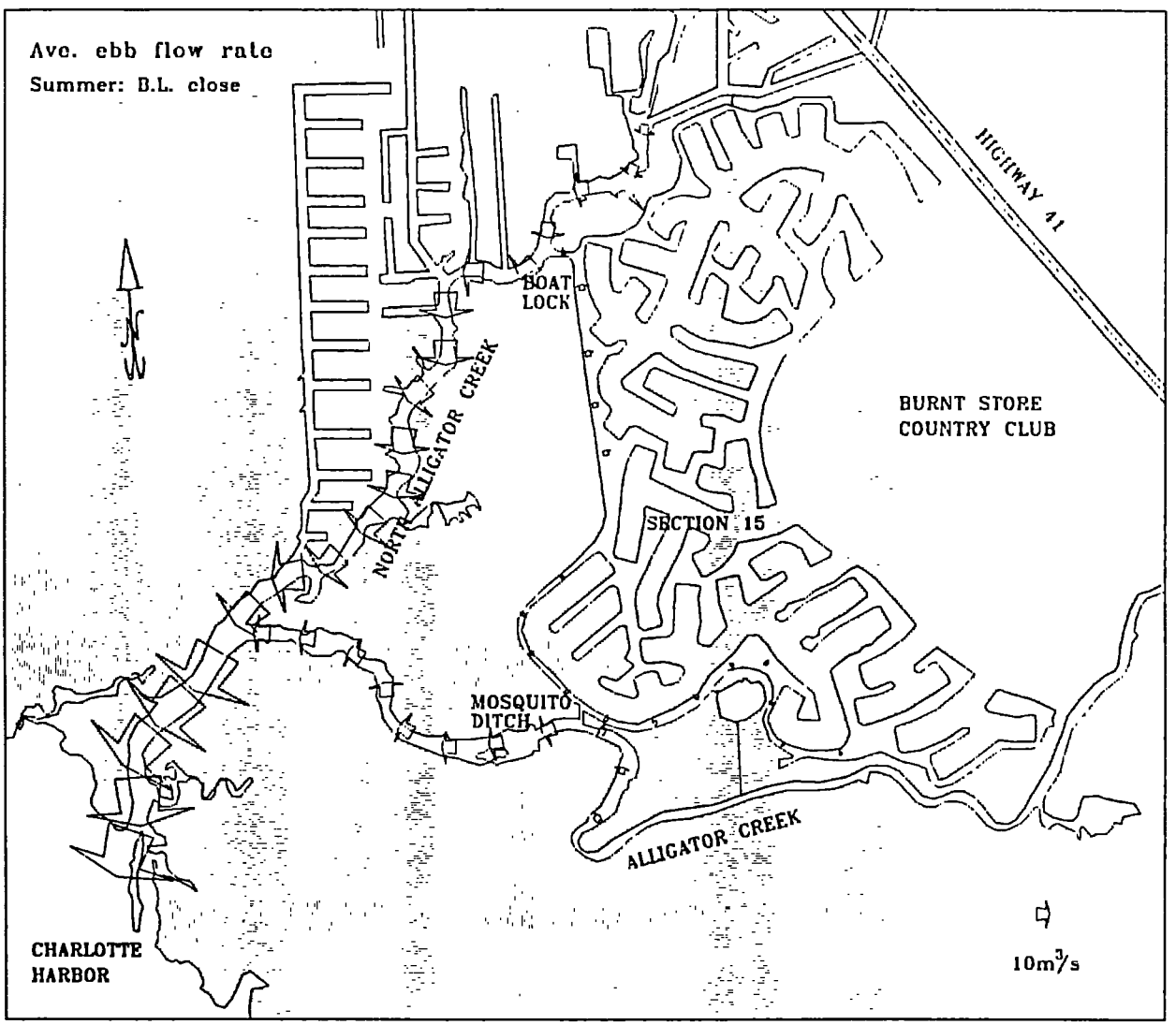

Figure 27: Time-averaged ebb flow pattern under lock-closed (summer) condition.

the shallow opening north of the boat lock. The total strength, however, is still considerably weaker than the lock-open condition. Consequently the stagnation zone is extended northward.

The non-dimensional plot of average gross flow rate for the three computational courses under lock-closed condition is given in Figure 28. The exchange through lock is now reduced to 16% but the exchanges through the mosquito ditch and north opening are increased to 25% and 9%, respectively. The combined contribution of 50% represents only 5% reduction compared with the lock-open condition.

b. Flow Under Winter Condition

The measured maximum ebb flow rates (from Table 2) were about -30 m^3/s at Station 7, -22 m^3/s at Station 6 and -7 m^3/s at boat lock. The maximum flood values were around 39 m^3/s at Station 7, 40 m^3/s at Station 6 and 14 m^3/s at boat lock. The Q–ΔH curves in Figure 13 are nearly symmetrical with respect to origin indicating nil stream flow during this winter period.

The results from the numerical simulation using the eight-day measured tide as input are shown in Figure 29. Since the measurement was taken during spring tide period the results roughly represent the peak tidal condition . Again, if the minor peaks are neglected, a representative of peak ebb flow at Station 7 is around -57 m^3/s; the peak flood flow is slightly less and around +47 m^3/s. The corresponding representative peak ebb and flood values at Station 5 are -31 and +25 m^3/s, respectively, and are -18 and +15 m^3/s at the lock, respectively.

The numerical results of the average ebb and flood patterns for lock-open case are shown in Figures 30 and 31. The flow patterns are similar to that of the summer condition. The non-dimensional gross flow rates along the three flow paths are shown in Figure 32. The exchange through the lock opening is 33% whereas the exchanges through the mosquito ditch and the north opening are 17% and 5%, respectively. Therefore, the sum of these three which represents the bulk of the exchange between Section 15 and the creek system amounts to 55% which is as same as the summer case. The section between K and L is exceedingly stagnant.

For the lock-closed condition, the flow rate is reduced but flow pattern remains the same as the lock-open condition. The non-dimensional gross flow rates are shown in Figure 33. The exchange rates through the lock, the mosquito ditch and the north opening are 18%, 26% and 9%, respectively for a total value of 53%. This represents 2% reduction compared with the lock-open condition.

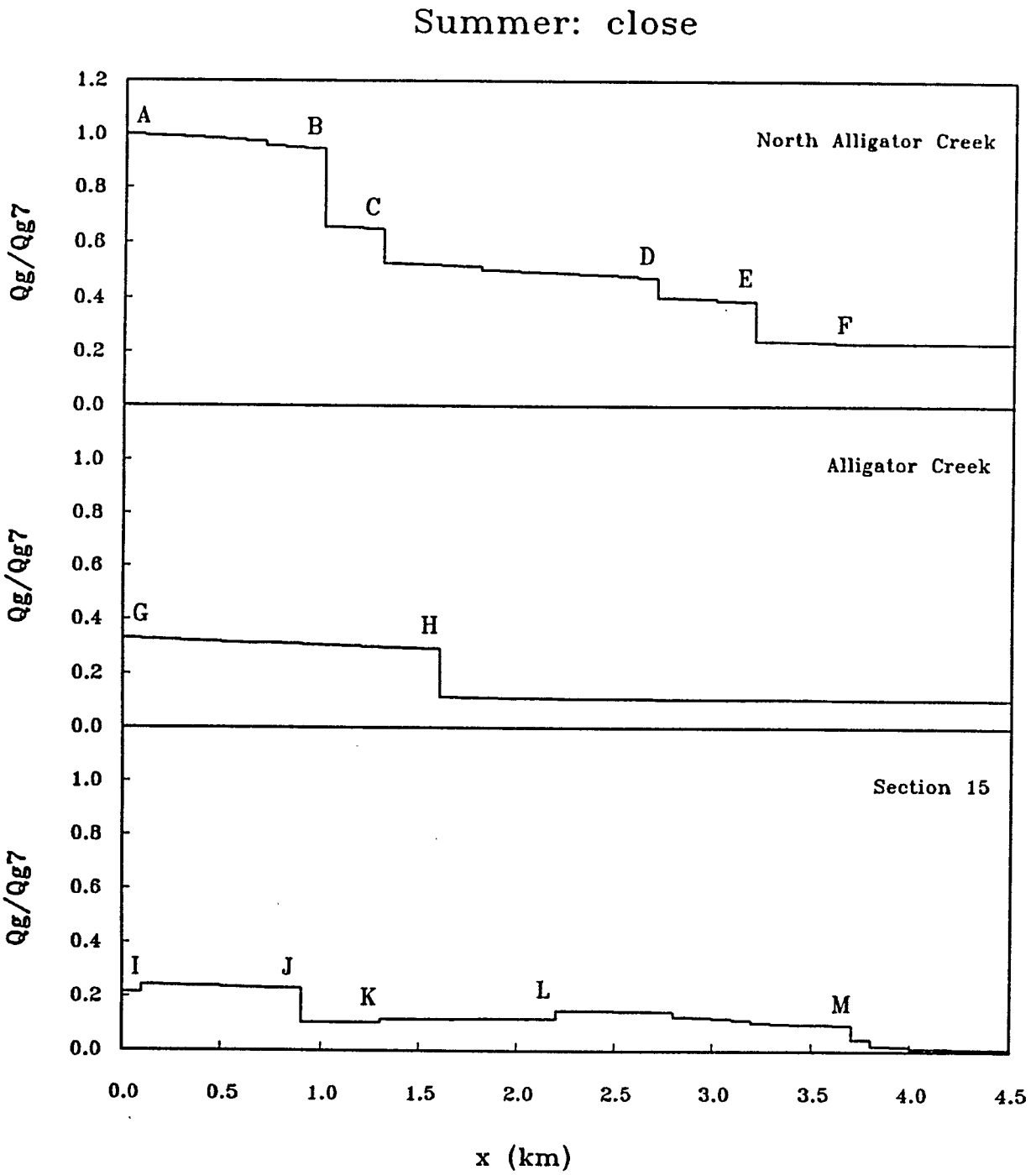

Figure 28: Non-dimensional plot of Q_g under lock-closed (summer) condition.

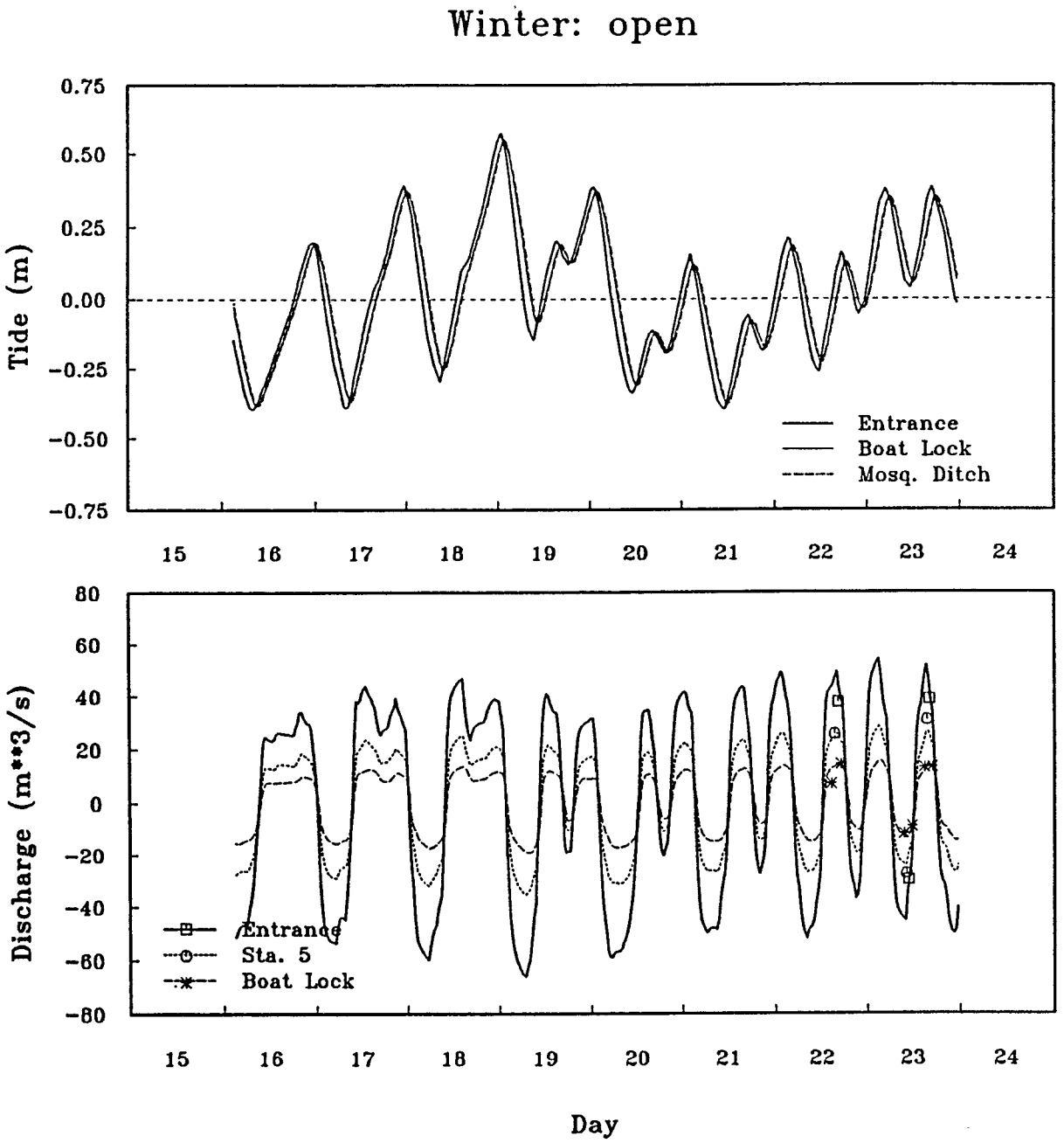

Figure 29: Simulation of tides and flow rates under lock-open (winter) condition.

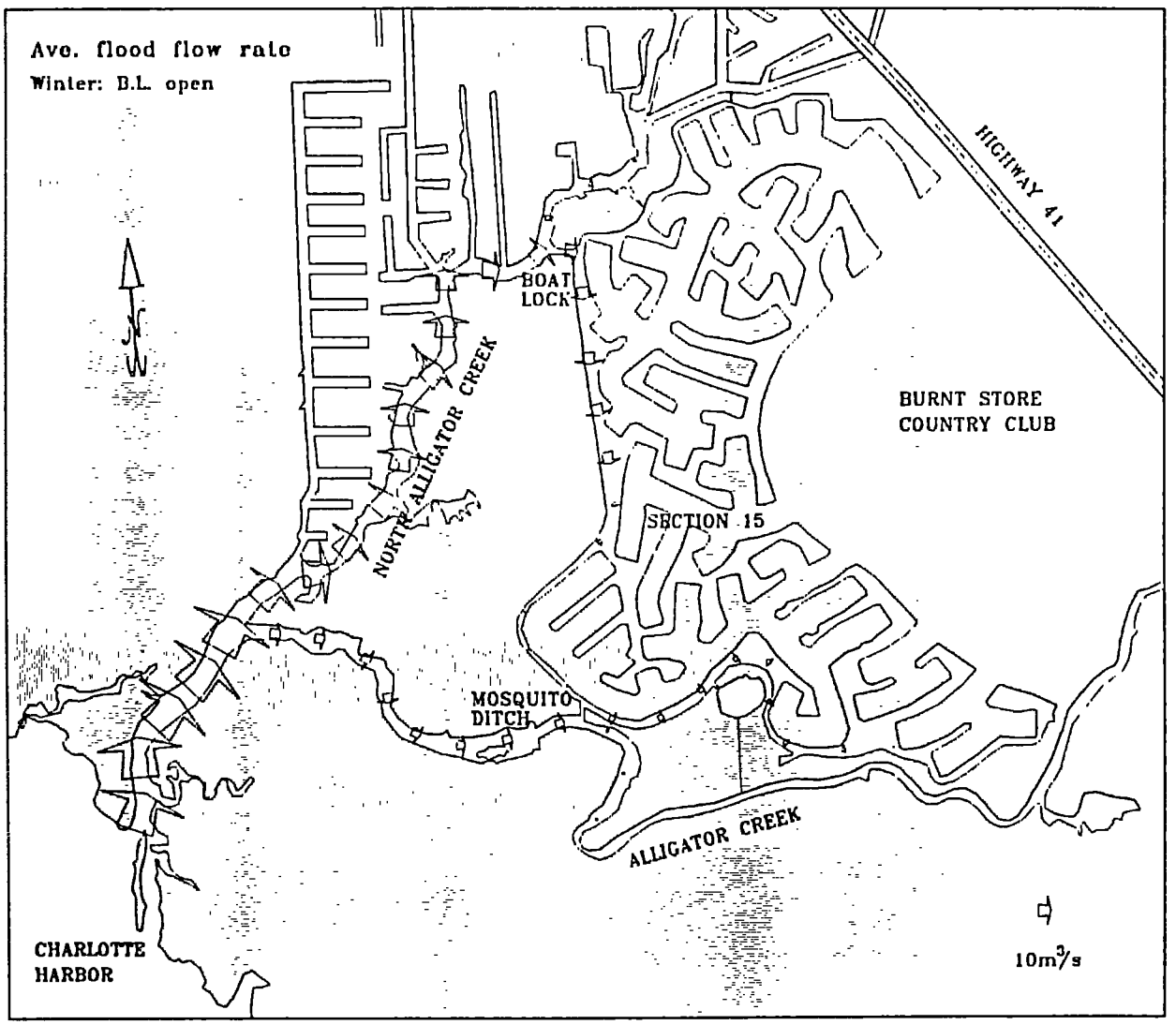

Figure 30: Time-averaged flood flow pattern under lock-open (winter) condition.

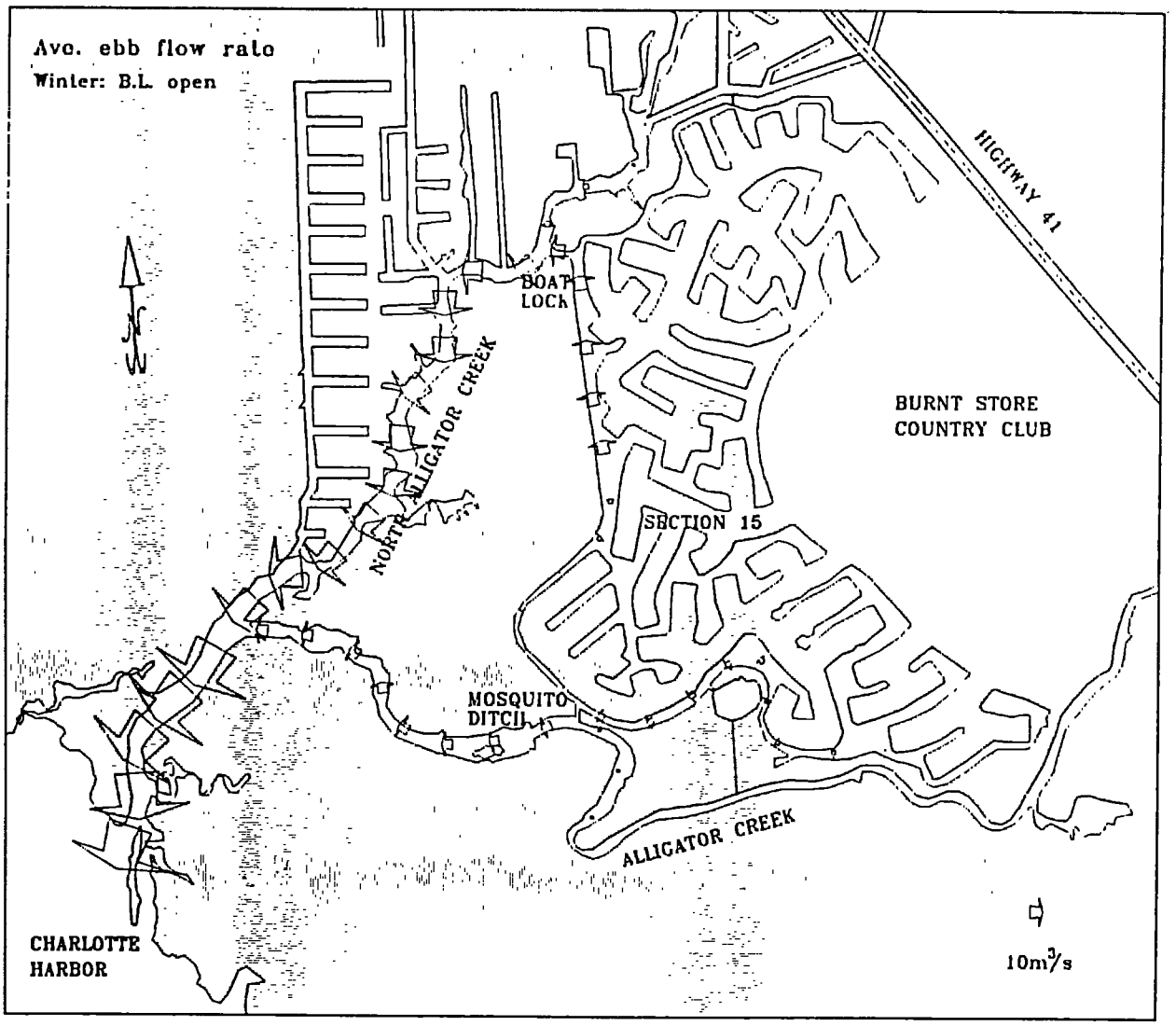

Figure 31: Time-averaged ebb flow pattern under lock-open (winter) condition.

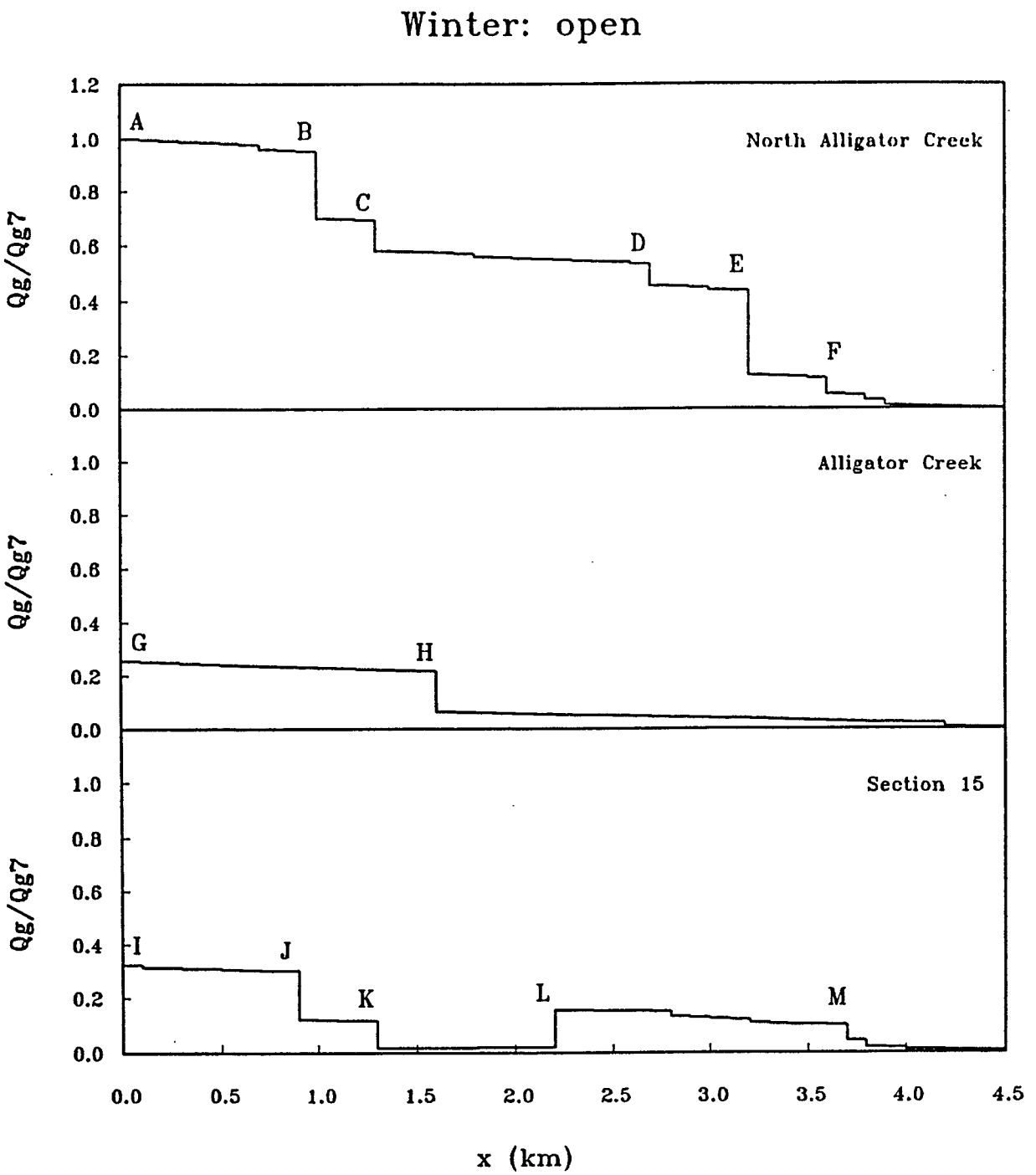

Figure 32: Non-dimensional plot of Q_g under lock-open (winter) condition.

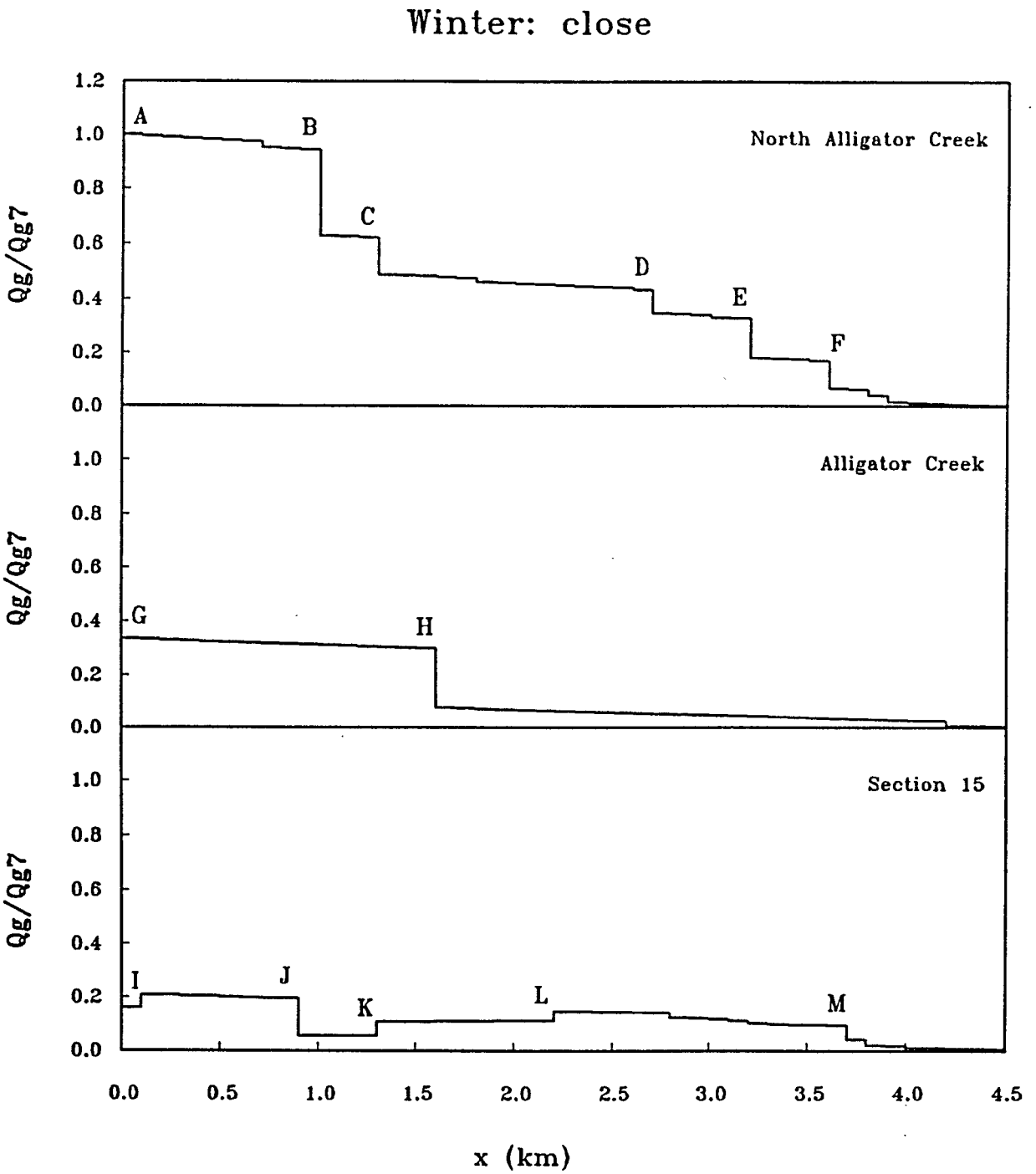

Figure 33: Non-dimensional plot of Q_g under lock-closed (winter) condition.

5.2 Boat Lock Effect on flow patterns in Section 15

Based on the results given above, it becomes clear that flow exchange between the canals in Section 15 and the creeks is mainly through three outlets. The south portion of the canal network covering about one-fourth of the total surface area exchanges water with the Alligator Creek through the mosquito ditch. The northern most portion of the canal network with little less than one-eighth of the total surface area exchanges water with the north branch of the Alligator Creek through the opening north of the boat lock. The central portion of the canal network with about five-eighth of the total surface area exchanges water with the north branch of the Alligator Creek through the boat lock. The discharge pattern is delineated in Figure 8 as three zones. There is very little interzonal exchanges as evidenced by the two stagnation sections separating the three zones. The central zone that exchanges water through the lock mainly consists of two separate canal networks; the upper network has the outlet to the trunk canal at the end of the Zafra Ct. and the lower network has the outlet between San Lorenzo Dr. and Macedonia Dr. The stretch of the trunk canal south of this outlet forms a bend and is identified as the stagnation section.

Under lock-closure condition, the stagnation section extends northward beyond the lower network outlet. Consequently, the complete lower canal network in the central zone becomes rather stagnant and the exchange with the lock is mainly from the upper canal network.

5.3 Sediment Transport

A secondary objective of the study is to make a quick assessment on the sediment and pollutant transport in the lock vicinity.

Sediment samples were collected from the bottom in the vicinity of the lock. The samples consisted of a significant amount of shell fragment. The remaining portions were mainly fine to median-fine sediment. Figure 34 shows the distributions of D_{50} in the lock vicinity region. As can be seen the values of D_{50} range from 0.14 to 0.2 mm. There is very little difference between summer and winter samples.

Under normal condition, one expects bed load to be the dominant mode of sediment transport. The following Bagnold-type equation can be used to estimate the transport rate:

$$I_b = 1000 \cdot W(u_* - u_{*,c})^3, \quad \text{in kg/s}$$

where W is the width of the lock section in m, u_* is the shear velocity and $u_{*,c}$ is the critical shear velocity.

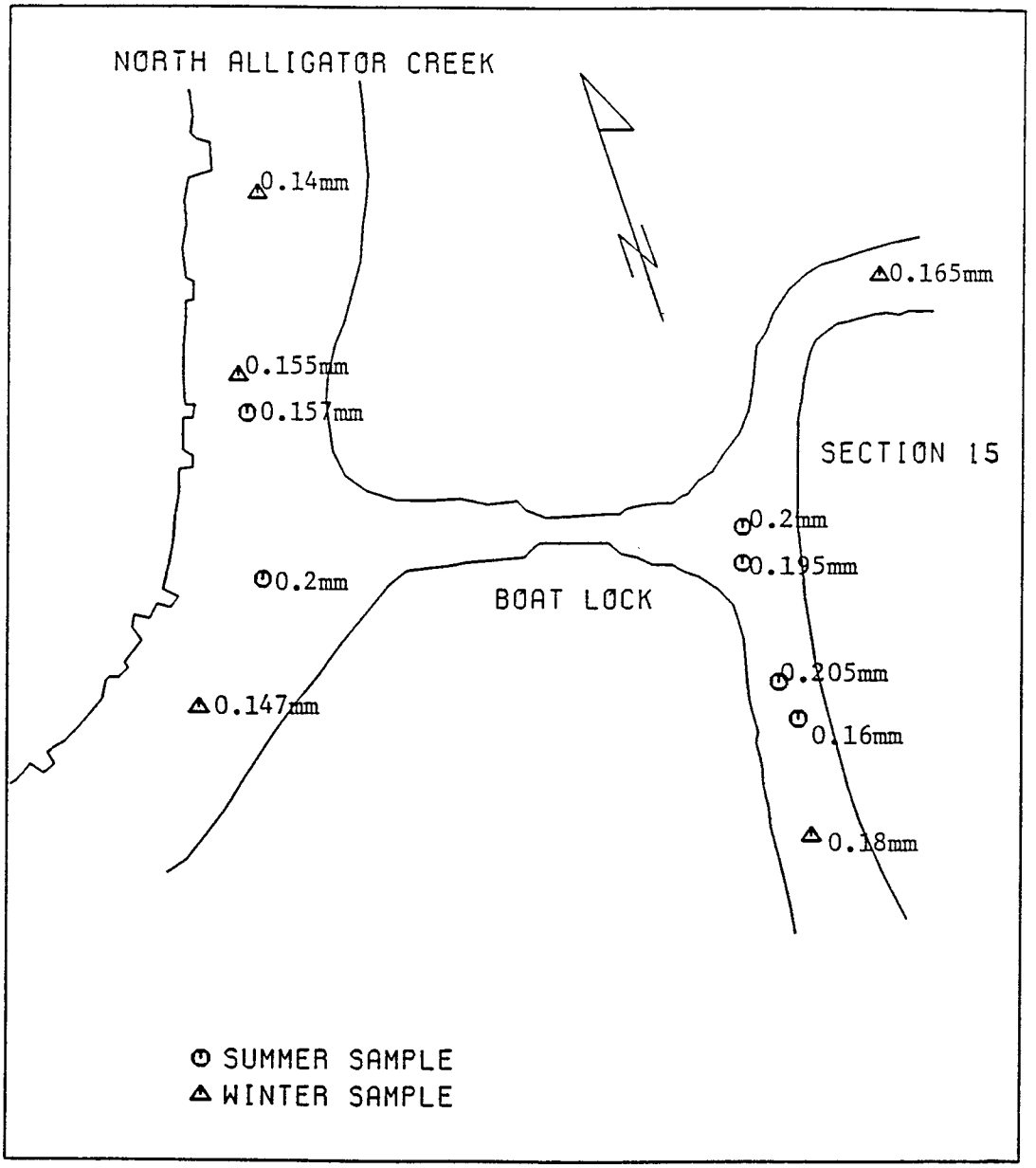

Figure 34: Distribution of D_{50} in lock vicinity region.

In terms of volumetric transport rate,

$$Q_b = \frac{(u_* - u_{*,c})^3}{(s-1)(1-p)} \quad \text{in m}^3/\text{s}$$

where s is the specific gravity of the sediment and p is the porosity of the sediment. For fine sediment, $u*, c$ is in the order of 0.01 m/s. The quantity u_* can be related to the mean stream velocity by the relationship:

$$u_* = \sqrt{f/8} \cdot \bar{u}$$

where f is the friction coefficient. Let f=0.02, s=2.6, p=0.4 and the peak ebb and flood velocity to be 0.5 m/s as measured and use the velocity time history as given in Figure 10, the average sediment transport rates per half tidal cycle (either flood or ebb) are estimated to be about 0.06 m^3/s for semi-diurnal tide and about twice as much for diurnal tide. The lock has a bottom width about 4 m. Thus, the sediment transported through the lock during half a tidal cycle is in the order of 0.25 to 0.5 m^3 depending upon semi-diurnal and diurnal conditions.

The accretion or erosion depends upon the net transport rate as well as the strength of the current. From the above calculation, one can see that if the mean stream velocity drops below 0.2 m/s, the region will basically become accretional. At the lock section, the mean velocity is considerably higher than 0.2 m/s and the ebb and flood velocities are almost symmetrical. Consequently, the lock section is non accretional. This also applies when the lock is closed as the bottom velocity under the lock remains strong.

Within Section 15, the stagnation section in the trunk canal is likely to experience severe shoaling. Most of the finger canals are also accretional as most of them behaves like reservoir during flood and ebb flows. Lock closure mainly affects the lower canal network in the central zone. It is not evident whether shoaling will be accelerated in this section which is dependent upon the net transport rate. Since the water becomes more stagnation under closure condition, the net direction of transport is difficult to determine. However, the outlet to the trunk canal is likely to be shoaled in as sediment carried in from the lock will be deposited at this location. One also expects that almost at every intersections along the trunk canal the shoal will be more prominent.

5.4 Pollutant Transport

Pollutant in the water column will be transported through current convection and turbulent diffusion. The magnitude and pattern of the tidal current have already established. The diffusion property in the lock vicinity was examined by a simple dye study. As discussed earlier, based on the results of the dye study and the

one-dimensional transport numerical model the longitudinal diffusion coefficient in the trunk canal was established as equal to 0.8 m^2/s. The value might be slightly higher in the creek system.

Based upon numerical model simulations pollutant passing through the lock section mainly affects the region shown as the shaded area in Figure 35. It includes two storage areas A and B in Section 15, two storage areas C and D outside along the north branch of the creek and the creek system itself. More detailed locations are marked on the map as grid location numbers from 1 to 41. The location #1 is at the entrance of the channel to the Harbor and location #41 is at the extreme south end of the trunk canal in Section 15. The grid locations #22 and #23 are the outlets of storages A and B, respectively, whereas #8 and #15 are the outlets for C and D, respectively.

Simulations were carried out for diurnal and semi-diurnal conditions with the lock open and with the lock closed. Some results for semi-diurnal tides are given here to explain the phenomenon. Since the main concern here is for pollutant originated from and in Section 15, the simulations are for pollutant released at locations #22 and #23, which represent those from the regions A and B.

Figure 36 shows the tracing of the pollutant for lock-open condition from the beginning of a flood tide. In the graph, the abscissa plots the grid locations from #1 to #41 with distance between two neighbouring locations equal to 0.5 km; the ordinate is the time with origin sets at the beginning of the flood tide. Thus, the six-hour mark roughly represents the end of the flood and the beginning of the ebb for the semi-diurnal condition and so on. The lines in each grid represents the percentage of pollutant at a specific location and time. Therefore, the darker the shade the higher the percentage. For pollutant originating from region A (#22), it is largely trapped in the trunk canal and storages A and B during flood. A small amount moves further southward through the mosquito ditch into the Alligator Creek. When the flow changes its direction in the ebb cycle, portion of the pollutant is being released from the storage and is carried out mainly through the lock. A significant portion of the pollutant is still trapped in the A and B. Diffusion appears to dominate convection in this portion of the canal as the flow is very slow. As a consequence the amount of pollutant escaped in the creek is small. At the end of the ebb, the centroid of the escaped pollutant reaches somewhere around location #4 which is about 1 km downdrift of the junction. A small portion of it enters into the Charlotte Harbor. As tide reverses to flood, the pollutant traces back to updrift with the main route following the north branch into Section 15. Therefore, the concentration in regions A and B increases periodically. Throughout the process, region B is the main trapping. Pollutant originating from storage B as can be seen has similar behavior.

Figure 37 shows the lock-closed condition for pollutant release at the beginning of a flood. Because of the reduced flow, the trapping time within the canal is

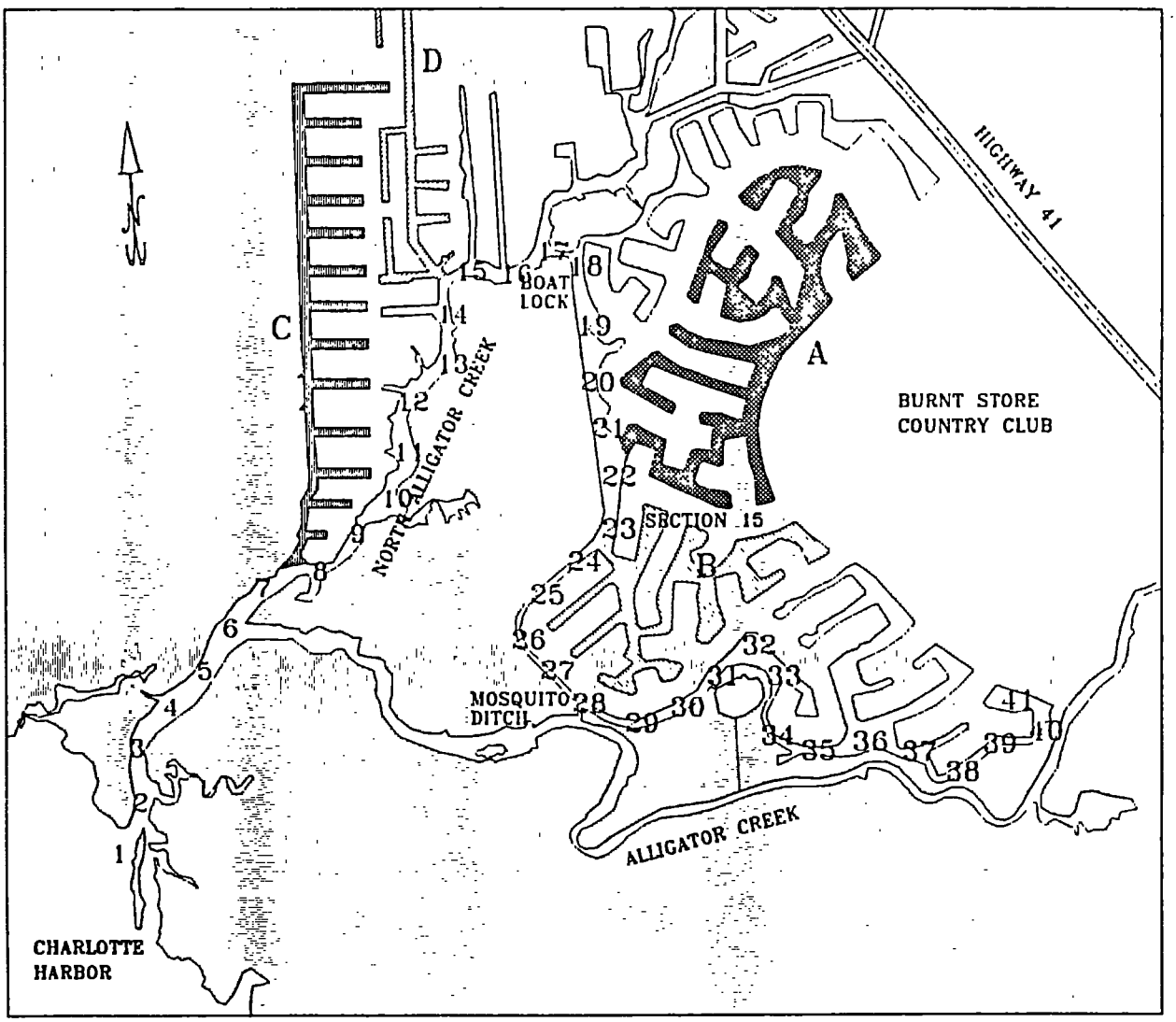

Figure 35: Regions affected by pollutant from Section 15.

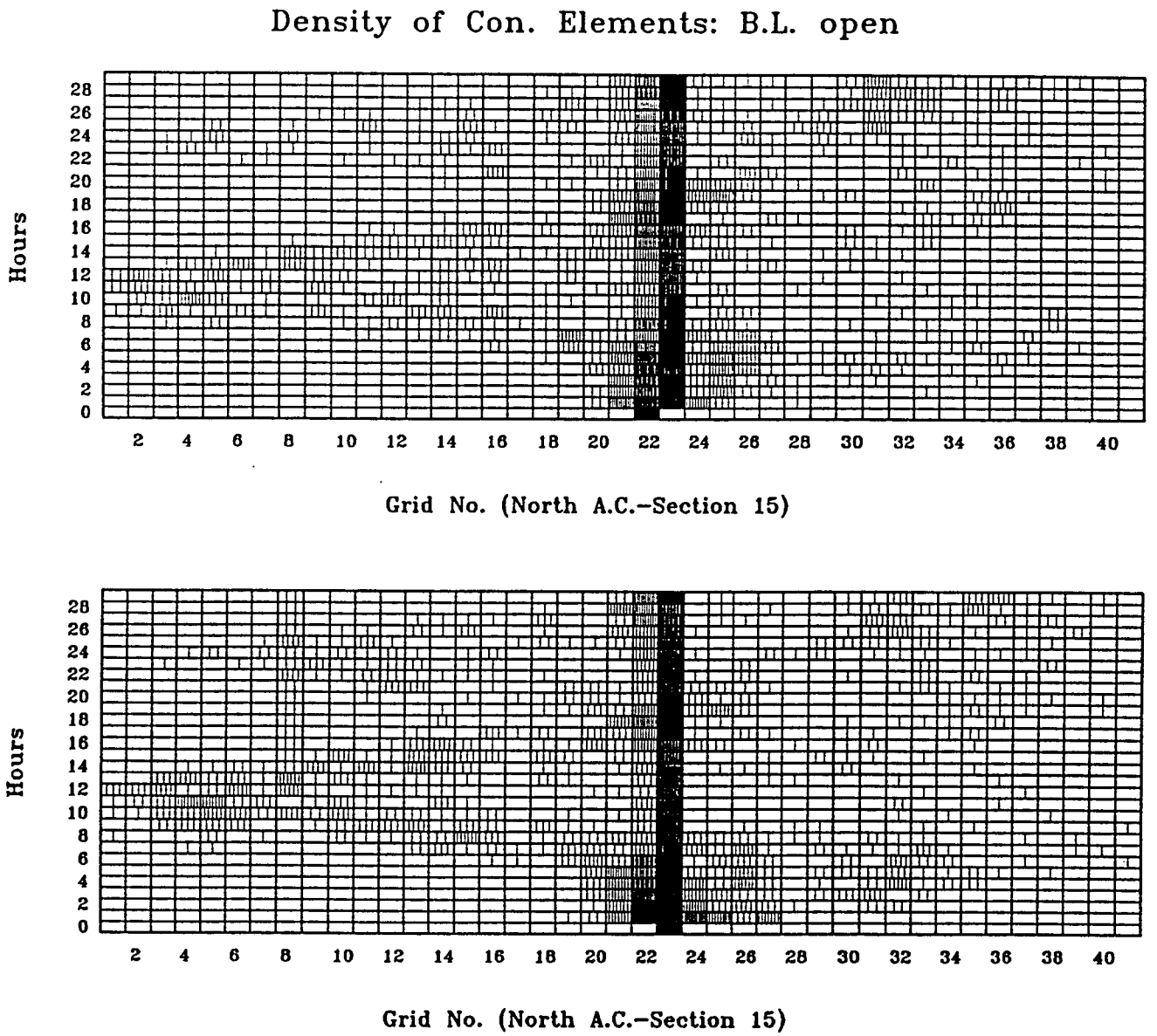

Figure 36: Temporal and Spacial variation of pollutant concentration under lock-open (flood) condition.

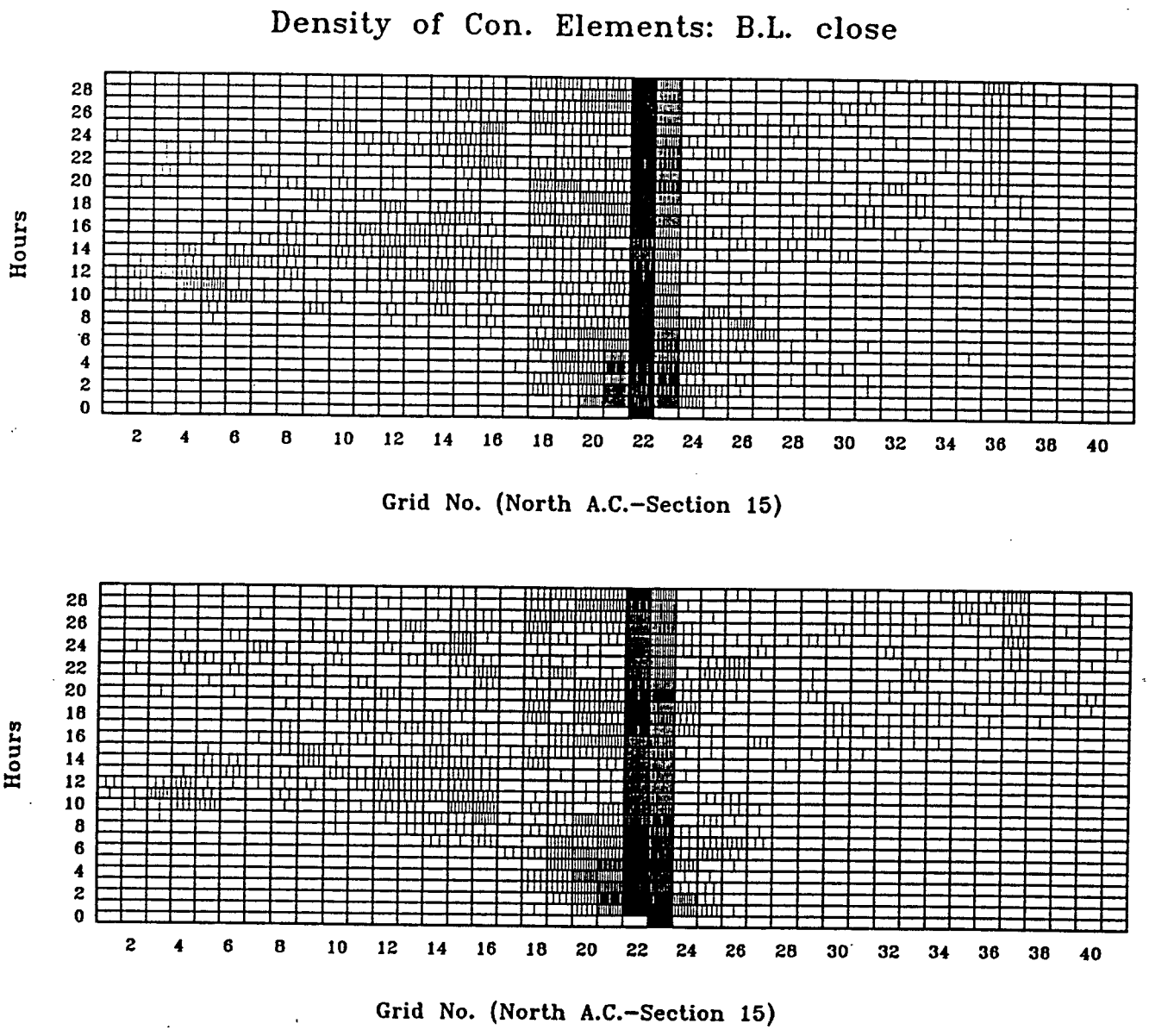

Figure 37: Temporal and Spacial variation of pollutant concentration under lock-closed (flood) condition.

increased. The pollutant eventually escapes through underneath the lock. The centroid of the pollutant now does not transport as far and all the storage areas along creek begin to trap the pollutant. Thus, closing the lock manages to trap the pollutant inside Section 15 longer. The pollutant eventually escapes into the north branch. Since the flow slower than the lock-open case the pollutant now resides longer in the storage areas along the creek. Another effect of closing the lock is the increased transport through the mosquito ditch. This is evidenced by the appearance of two centroids along the creek near the end of ebb tidal cycle (10–12 hours). One centroid located upstream near locations #14 and #15 is due to the pollutant originating from the lock and the other centroid located downstream near the junction around #4 and #5 is due to the transport through the mosquito ditch. The total quantity escaped from Section 15 does not appear to have diminished significantly by closing the lock.

Now, for pollutant release at the beginning of ebb condition, Figure 38 shows the lock-open case. Here, the pollutant immediately transports into the Creek through the lock. The location of the centroid at the end of the ebb is roughly the same as the flood release but the concentration is now increased. As the flow reverses to flood the pollutant retraces its path back to Section 15. More pollutant is being trapped in storage areas along the creek. Again, storage B is the main trapping of the system. For the lock-closed case (Figure 39), the transport through the lock is delayed but the delay is not long enough to prevent the pollutant from eventually escaping to the creek before the ebb tide is over. The transport through mosquito ditch increases. Storage A now becomes the main trapping as stagnation zone in the trunk canal extends further north.

The total pollutant dilution in Section 15 for lock-open and lock-closed conditions are simulated using January tidal record as the input. The results are shown in Figure 40. The pollutant is released initially at location #22 at beginnings of flood and ebb, respectively. For flood release, the pollutant initially disperses inside Section 15 while being trapped by the flood flow. Therefore, the rate of dilution is slower. For ebb release, the pollutant is being transport out of Section 15 considerably faster than the flood release case. The lock-open and lock-closed conditions, on the other hand, have only minor influence on pollutant transport in Section 15.

Like the flow exchanges, the boat lock is mainly responsible for pollutant exchanges from the central zone of Section 15 to the north branch of the Alligator Creek. The two end zones have different outlets. The flow exchanges among three zones are minor in single tidal cycle. The diffusion process, of course, eventually produces mixing of pollutants originating from different locations.

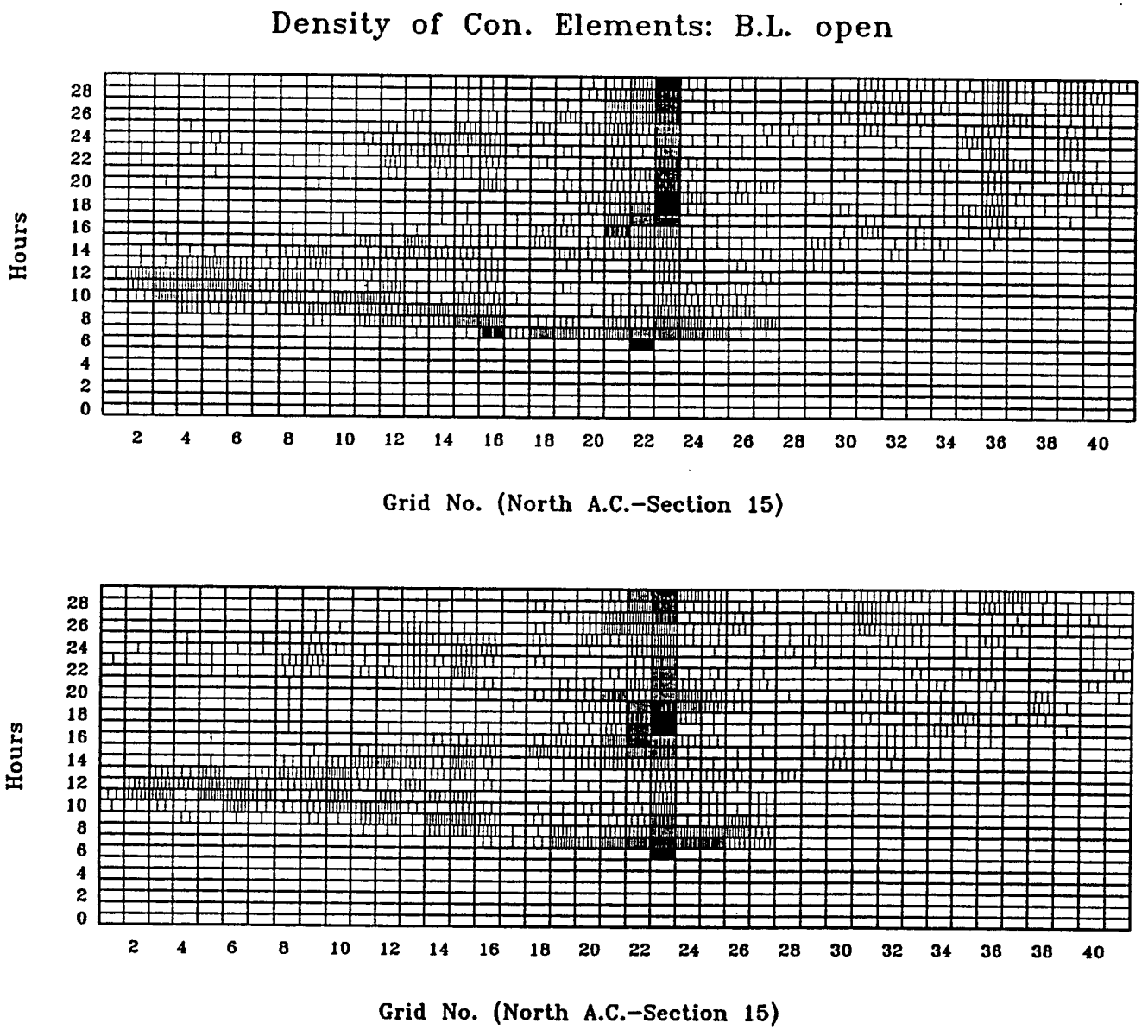

Figure 38: Temporal and Spacial variation of pollutant concentration under lock-open (ebb) condition.

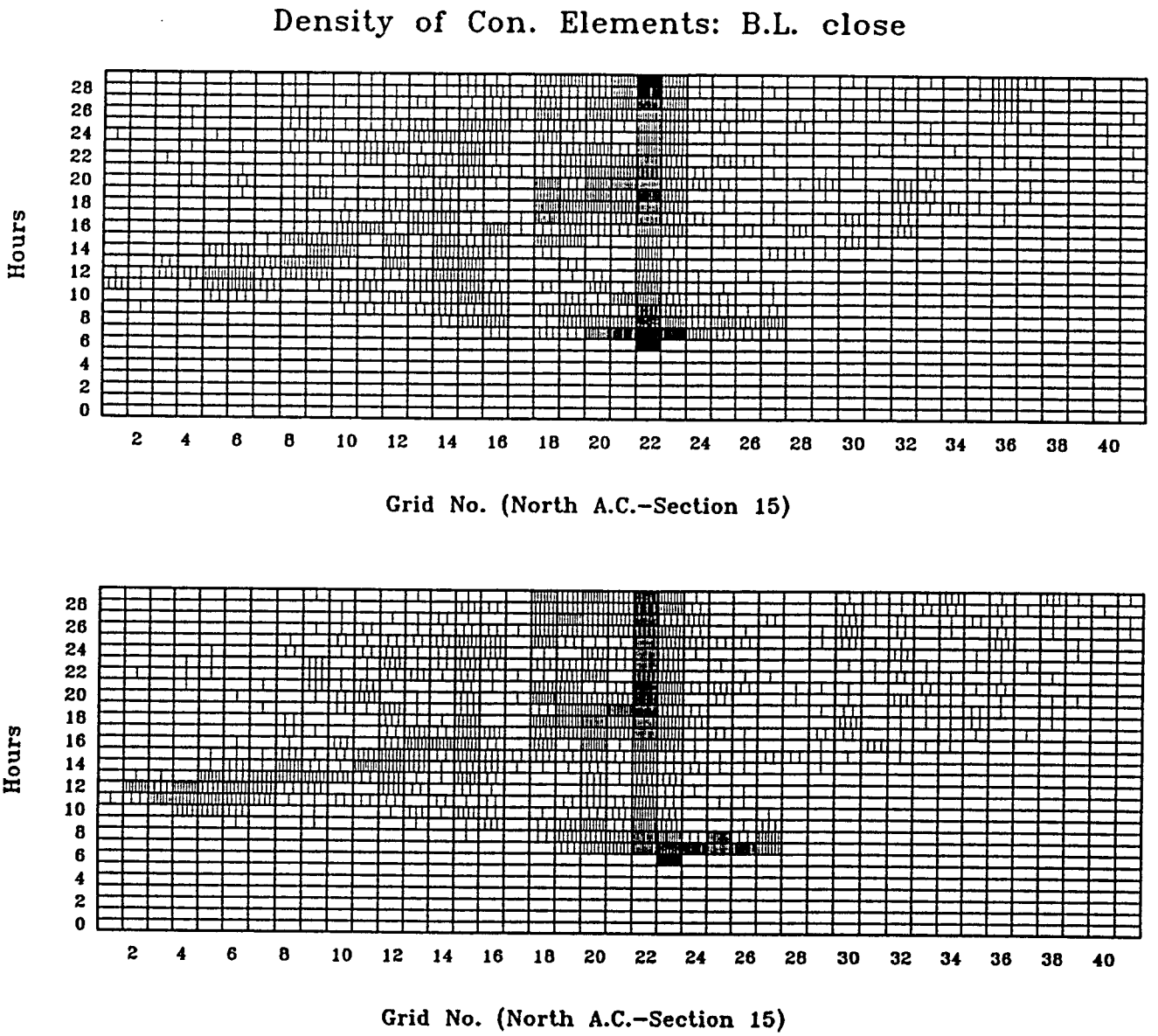

Figure 39: Temporal and Spacial variation of pollutant concentration under lock-closed (ebb) condition.

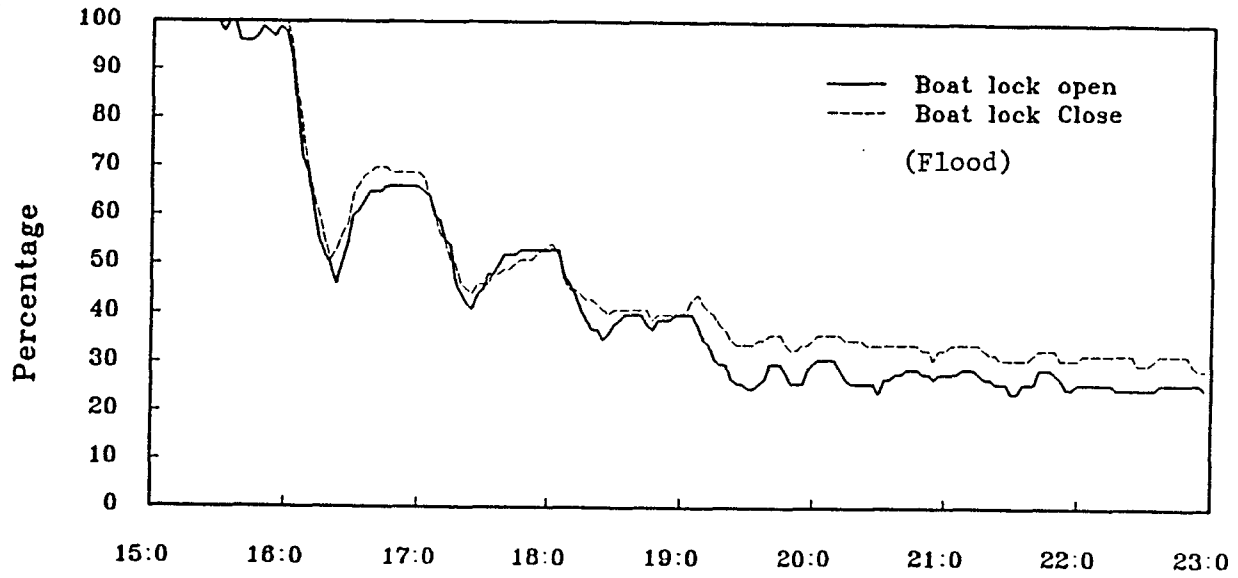

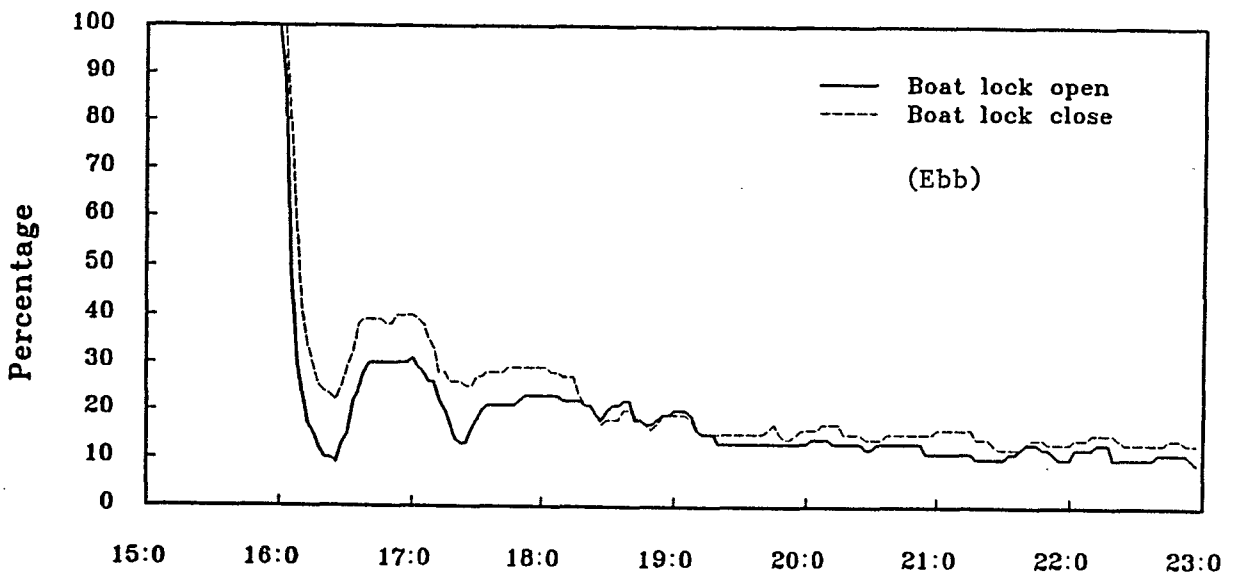

Figure 40: Simulation of total pollutant dilution in Section 15.

6 Summary and Conclusions

6.1 Summary

A field measurement study augmented with numerical modeling was carried out for the determination of the flow and transport characteristics for a section of the Punta Gorda municipality that contains the Burnt Store Isles subdivision. The emphasis of the study is to assess the effects of the boat lock closure (or opening). Some of the major findings are summarized here:

1. Flow Characteristics

- The entire flow network of which Section 15 is an integral part is tidal dominated. The tidal action is a mix of diurnal and semi-diurnal. Spring tide condition is usually associated with the diurnal component. The spring tidal range is in the order of 1 m. Based upon field measurement, the stream discharge was in the order of 10 cu m/s in the summer season and was negligible in the winter. About 65% of the stream discharge originated from the north branch of the Alligator Creek and the rest 35% from the Alligator Creek. The ratio of this summer stream discharge to the time averaged tidal induced flow volume entering the network is about 1 to 3.

- There are three main outlets in Section 15, the boat lock in the middle, a mosquito ditch on the southside and a shallow opening north of the boat lock. The south 1/4 of the canal network exchanges water with the Alligator Creek through the mosquito ditch. The northern most portion of less than 1/8 of the area uses the shallow opening as the outlet. The central portion of the canal network with about 5/8 of the total surface area exchanges water with the north branch through the lock. There is very little interzonal exchange.

- It was estimated here that leakage through boat lock when closed is about 15% of boat lock-open condition.

- The flow entering Section 15 through the three openings is almost entirely due to tidal-induced flow. Only an insignificant amount of stream flow from the upper north branch gets diverted into the trunk canal in Section 15 via the lock and discharges back to the Alligator Creek through the mosquito ditch.

- . Using time averaged gross flow rate as a reference and discounting the stream discharge, about 55% of the tidal induced flow enters and leaves Section 15 in lock-open condition. This ratio is the same for winter and summer. For lock-closed condition, this value reduces slightly to about 50%

and 53% for summer and winter, respectively. The net difference is 3.5% for lock-open and lock-closed conditions.

- For lock-open condition, about 32% of the tidal induced flow flows through the boat lock in both summer and winter seasons and this percentage reduces to 18% for lock-closed condition. Therefore, the reduction of flow through the lock is 14%. However, this reduction is largely made up by the increase of flow rate through the mosquito ditch and the north opening when the lock is closed. The net reduction of flow from Section 15 as a whole is 3.5% as given in the previous paragraph.
- There is a stagnation segment in the trunk canal starting from the Macedonia drive and extending southward around a bend. For lock-closed condition, this stagnation segment extends further north to Zafra Ct.

2. Sediment Transport

- The bottom sediment near boat lock can be classified as fine to median fine sand with a fair amount of shell fragment.
- The average sediment transport rate per half tidal cycle (either flood or ebb) through the lock is estimated to be in the order of 0.25 m^3 for semi-diurnal cycle and double of that for diurnal cycle.
- The lock section will remain clear with no shoaling problem whether the lock is open or not. The stagnation zone in the trunk canal identified earlier and those finger canals with outlets to the trunk canal within this zone are likely to experience severe shoaling. Of course, the shoaling will extended further north if the lock remains closed.

3. Pollutant Transport

- Pollutant transported through the lock opening affects the north branch of the Alligator Creek and four main storage areas, two in the central zone of Section 15 and the other two along the north branch. The two end zones in Section 15 have different outlets.
- Under lock-open condition, pollutant released from the central zone of Section 15 finds its way downdrift through the lock during ebb cycle. The centroid of pollutant at the end of the ebb tidal cycle will be located about 1 km downdrift from the junction of the two creeks if the tide is semi-diurnal. For diurnal tide, the centroid will escape the channel and enter the Harbor. When tide reverses under semi-diurnal condition, pollutant traces back into Section 15 causing the level of pollutant to increase again. Storage B is main trapping for the system.

- Under lock-closed condition, pollutant released from the central zone of Section 15 has a longer resident time in the trunk canal in the order of two to three hours as compared with the lock-open condition. However, this resident time is not long enough to trap the pollutant in the canal network. Therefore, at the end of the ebb tide, semi-diurnal or diurnal, part of the pollutant will be outside the lock but its location will be further upstream compared with the lock-open condition. Consequently, during tidal reversal, the pollutant will fill more storage areas along the north branch than the lock-open condition and move upstream beyond the lock. The total pollutant transport through the lock will be reduced by a small amount. However, this reduction is largely compensated by the increase of transport through the mosquito ditch to the Alligator Creek proper. The pollutant transport appears to be consistent with the flow condition discussed earlier.

6.2 Conclusions

The boat lock is responsible for water and pollutant exchanges for the central 5/8 portion of Section 15. In terms of time averaged flow rate, by closing the boat lock the contribution from Section 15 to the total discharge realizes a mere 3.5% reduction. Since the flow in Section 15 is tidal dominated, the seasonal effects on lock closure is negligible in terms of discharge from Section 15.

Based on the study results, the boat lock is ineffective of trapping either sediment or pollutant within Section 15. The reduction of pollutant transport is largely made up by the increased transport from the mosquito ditch. Closing the boat lock for an extended period will likely accelerate shoaling in the central portion of the trunk canal and its connecting finger canals. Also, closing the boat lock will likely to increase the average resident time of pollutant in the storage areas along the creek and to cause the pollutant to transport further upstream along the north branch.

The storage areas (finger canal sections) and portion of the trunk canal are rather stagnant, thus, conducive to shoaling and pollutant trapping.

The above conclusions are based on a small amount of field data collected under normal summer and winter conditions. The numerical model is based on simplified assumptions and limited calibrations. Therefore, the results should be viewed within this context.

The numerical results revealed that the entire system is a sensitive one. Variations of input conditions or alternation of outlets could result in significant changes of flow conditions as well as the pollutant and sediment transport patterns. As an example, storage B is the main trapping segment under lock-open condition.

Under lock-closed case, the entire Section 15 is readjusted causing increased flow from other openings and the main trapping area shifted to storage A.

The study is of limited scope. The actual sensitivity of the system is not established. The system may also behave differently under extreme conditions such as summer storms, hurricanes or other episodic events.

The numerical model should prove to be a very useful tool for improving the system. It is recommended to further refine the model; to collect more field data of longer term and eventually to expand the model to cover the other regions in the City.

References

[1] Chorin, A.J. 1978. "Vortex Sheet Approximation of Boundary Layer," Journ. of Comput. Phys., Vol.27, PP.428-442.

[2] Ippen, A.T., 1966. "Estuary and Coastline Hydrodynamics," McGraw Hill Inc.